JOURNAL OF MATERIALS SCIENCE 29 (1994) 1135–1158

Review
Rare-earth chalcogenides – an emerging class of optical materials

P. N. KUMTA
Department of Materials Science and Engineering, Carnegie Mellon University, Pittsburgh, PA 15213, USA

S. H. RISBUD
Division of Materials Science and Engineering, University of California, Davis, CA 95616, USA

Sulphide compounds belong to the family of chalcogenides and are well known for their optical and electronic properties. They possess good optical properties because of their ability to transmit into the infrared (IR) region. Several sulphide glasses are known to exist which exhibit far infrared transmission and are also useful semiconductors. In recent years, there has been an increasing interest in IR materials to be used on surveillance equipment. This led to the identification of several new crystalline sulphide materials which can transmit very far into the IR region (up to a wavelength of 14 μm). Crystalline and amorphous rare-earth sulphides emerged as a new class of materials, which possess several unique optical and electronic properties. This paper reviews the status of these rare-earth sulphide amorphous and polycrystalline materials, the techniques used to process these materials and discusses their structure, thermal, mechanical and optical properties. Conventional and emergent novel chemical processing techniques that are used for synthesizing these materials are reviewed in detail. The use of metallorganic precursors and the modification of their chemistry to tailor the composition of the final ceramic are illustrated. The potential of these chemical techniques and their advantages over the conventional solid state techniques used for processing sulphide ceramics is discussed, particularly in light of their successful applications in processing novel electronic and optical oxide ceramics.

1. Introduction

Sulphide compounds belong to the family of chalcogenide materials which are essentially compounds containing sulphur, selenium or tellurium. These compounds have received considerable interest over the years because of their glass-forming ability and interesting optical, electrical and acoustic properties [1–3]. Active research conducted in the area of non-oxide glasses in the last four decades has resulted in the identification of several new glass-forming systems, while the search for new materials with combined transmission properties and high-temperature stability led to the recent interest in the crystalline rare-earth sulphides. The rare-earth sulphide materials constitute a special category of the chalcogenides. The excellent thermal stability, strength and infrared (IR) transmission characteristics of the rare-earth sulphides also made them good candidates to be studied for glass formation. This paper reviews the processes used in synthesizing the amorphous and crystalline rare-earth sulphides and discusses their properties in two sections. The first section discusses the origin and nature of the chalcogenide glasses and the evolution of rare-earth sulphide-based glasses. Several rare-earth-based glass systems will be discussed and their properties highlighted. The second section describes the processing of crystalline rare-earth sulphides and discusses their structure and properties.

2. Chalcogenide glasses

Chalcogenides are compounds whose anions belong to group VI of the Periodic Table i.e sulphur, selenium and tellurium. In amorphous systems, this term is used rather routinely to differentiate sulphide, selenide and telluride glasses from oxide glasses. Most chalcogenides form glasses very easily and several glass-forming systems have been identified containing these elements and combinations of several other elements [1, 4, 5]. The glasses are well known for their optical and electronic properties. The electronic properties of the glasses arise from the changes in the electrical conductivity. At a certain specific voltage, the chalcogenide glasses undergo structural change and the glasses "switch" to a higher conduction state. This change in conduction can be several orders of magnitude and is useful in switching circuit devices. If the structural change is irreversible, then crystallization would occur causing memory switching [6].

0022–2461

The optical properties of these glasses originate from the characteristic low vibrational frequencies of the M–S (M = metal) bond rendering the glasses transparent in the long wavelength spectral region, in contrast to the oxide glasses. Some of the well-known glasses in the chalcogenide group of compounds are As_2S_3, GeS_2, $GeSe_2$, and several glass-forming compositions in the Ge–Sb–S, Si–Ge–As–Te, Ge–P–S, systems, etc. Table 1 shows some important chalcogenide glass systems and their applications. The excellent glass-forming ability of the chalcogenides originates from the large size of the anions which can combine with other elements to form glasses in a wide range of proportion. The glass-forming tendency in these glasses decreases in relation to the various elements as S > Se > Te, As > P > Sb, Si > Ge > Sn, while the nature of the transmission of these glasses typically decreases as Te > Se > S.

Since the early studies on As_2S_3 in 1950, considerable progress has been made in the development of sulphide glasses from that time until today. Several new glass-forming compositions have been developed, and studies on the optical, electrical and structural properties have identified them to be suitable for various applications, such as optical fibres, semiconductor devices, and optical windows. Table II lists the optical and thermal properties of chalcogenide glasses. They are covalently bonded materials and form glasses with long chain networks containing covalent metal–metal and metal–chalcogen bonds. The low bond strengths of these materials suggest the weak nature of the chalcogenide bonds which explains their low softening points and high coefficient of thermal expansion. On the other hand, the large size of the chalcogens and their weak bond strengths give rise to low vibrational frequencies, and hence, these glasses exhibit very good transmission into the infrared (IR) [6, 7].

It is now well established that the ability of a material to exhibit long wavelength transmission is dependent not only on the material possessing a large band gap, but is also governed by the vibrational frequency (ν) of the cation–anion bonds resulting in the IR absorption cut-off. The disordered structure of the glass makes the accurate calculation of this frequency, ν very difficult and only estimates can be made from the frequency relationship given by

$$\nu = \frac{1}{2\pi}\left/\frac{k}{M}\right\sqrt{}^{1/2} \quad (1)$$

where M is the reduced mass for two bodies, m_1 m_2, vibrating with an elastic restoring force constant k, expressed as

$$M = \frac{m_1 m_2}{m_1 + m_2} \quad (2)$$

Accurate evaluation of these frequencies in amorphous systems becomes difficult because of the perturbations caused by the influence of several other constituents in the structure. Another factor governing the transmission characterisitics of glasses is the respective field strength, Z/r^2, were Z is the ionic charge and r is the crystal ionic radius. Table III lists these values for ions that participate in a glassy network. Typically, glasses containing larger anions and cations with lower field strengths tend to form glasses that transmit well into the infrared. Dumbaugh [8] has given a good account of these conclusions and other properties of various glass-forming compositions. However, lower field strengths and weaker chemical bonding generally helps the transmission of the material into the long wavelength regime but at the cost of poor physical and chemical properties. Table II lists the properties of some typical chalcogenide glasses, while Fig. 1 shows the transmission characteristics of some oxide and non-oxide glasses. The chalcogenide glasses clearly display long wavelength transmission characteristics, in contrast to the oxides.

Several chalcogenide glass compositions have been researched and studied over the past three decades since the fabrication of As_2S_3, which was the first glass of this type to find commercial application. Arsenic trisulphide, As_2S_3, was first reported in 1870 when its potential for infrared transmission was identified, but extensive research into the determination of its structure and properties was not performed until the early 1950s. It has been used as an optical component in the

TABLE I List of some important chalcogenide glass systems and their applications

Glass systems	application
I. Electronic glasses	Switching circuits
As_2Te_3	
Si–Ge–As–Te (STAG)	
Ge–Sb–S–Te (ECD)	
$Ge_{15}Te_{81}Sb_2S_2$	
$(SiAsTe)_{95}P_5$ (SPAT)	
$Ge_{33}As_{17}S_{15}Te_{35}$(GAST)	
II. Optical glasses	Materials for photocopiers
Se, selenide glasses	
In_2S_3,Y_2O_2S,La_2O_2S	Phosphor application
As–S, Ge–S, Ge–P–S	IR transmission
Ge–Te, Ge–Sn–Te	Optical recording
III. Sonic glasses	
Ge–As–S	Acousto-optic application

TABLE II Optical and thermal properties of some important chalcogenide materials

Material	Transmission range (μm)	Refractive index at 3 μm	Thermal expansion (10^{-6} °C^{-1})	Glass transition temperature (°C)
Chalcogenides				
ZnS	0.5–12	2.2	7.5	–
ZnSe	0.6–14	2.4	7.6	–
Sulphide glasses				
As_2S_3	0.6–10	2.4	25	210
GeS_2	0.5–10	2.0	13	–
Ge–Sb–S	0.5–22	–	–	320
Selenide glasses				
As_2Se_3	0.7–15	2.7	21	200
$GeAs_2Se_7$	0.7–15	2.6	19	≈ 250
Telluride glasses				
$GeAs_2Te_7$	0.5–18	2.9	18	178

TABLE III Mass and field strengths of glass-forming ions

Element	Charge, z	Mass, m	Radius, r (nm)	Field strength, z/r^2
B	+3	11	0.023	57
P	+5	31	0.035	41
Si	+4	28	0.042	23
Be	+2	9	0.035	16
Ge	+4	73	0.053	14
Al	+3	27	0.051	12
As	+3	75	0.058	8.9
Ga	+3	70	0.062	7.8
Hf	+4	179	0.078	6.6
Zr	+4	91	0.079	6.4
Sb	+3	122	0.076	5.2
Te	+4	128	0.102	3.8
Th	+4	232	0.102	3.8
Bi	+3	209	0.096	3.3
Pb	+2	207	0.120	1.3
N	−3	14	0.171	1.03
O	−2	16	0.132	1.15
S	−2	32	0.184	0.59
F	−1	19	0.133	0.57
Se	−2	79	0.191	0.55
Te	−2	128	0.211	0.45
Cl	−1	35	0.181	0.30
Br	−1	80	0.196	0.26
I	−1	127	0.220	0.21

[a] Extracted from [8].

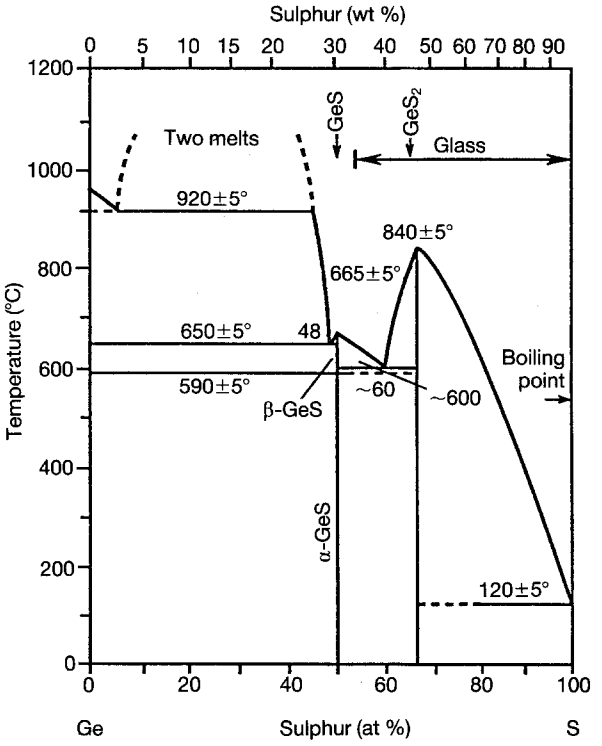

Figure 2 Glass-forming regions in the germanium (Ge)–sulphur (S) system. Structural differences can be seen in the glasses depending on the sulphur contents and the cooling conditions. Refer to the text.

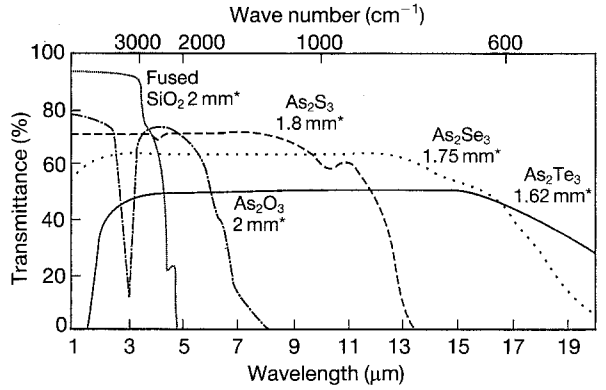

Figure 1 Transmission characteristics of some oxide and non-oxide glasses. Note the long wavelength transmission cut-offs of sulphide, selenide and telluride glasses in comparison to the oxides. (*) thickness.

3–5 μm window region primarily because of its infrared transmission, although there are several other glass-forming systems which transmit well into the mid- and far-infrared spectral regime as shown in Table II. Binary germanium sulphide glasses are also well known for their application in the mid-infrared region. For the germanium-sulphur system, the glass forming region is shown in Fig. 2. Although the entire region beyond 55 at % S is shown to be glass-forming, the actual boundaries are strongly dependent on the cooling conditions, and correspondingly, there are structural differences in the glasses [9, 10]. In the region corresponding to 66.7 to 90 at % S, the structure of the glasses is believed to be based on a three-dimensional inorganic polymer with chains of sulphur cross-linked with germanium and, in the region containing 56.7 to 60 at%, the structure of the glass is analogous to the silicate system. Since its first study in 1969, several researchers have investigated these glasses in detail to determine the exact glass-forming domain, its structure and its applicability in infrared fibre optics. While considerable research has been performed on the chalcogenide glasses little is known about the rare-earth sulphide-based glasses.

2.1 Rare-earth sulphide-based chalcogenide glasses

The rare-earth sulphides, unlike the common chalcogenides, are refractory solids and the cubic forms of these compounds also exhibit long wavelength transmission, as confirmed from our on-going work on γ-La_2S_3[11–15]. They are thermally stable with high melting points, and are mechanically strong with moderate expansion coefficients. The rare-earth sulphides (La–Er) are not glass formers but form reasonably stable glasses when mixed with other chalcogenide glass-forming sulphides such as gallium sulphide, germanium and arsenic sulphide. Glasses containing several rare-earth sulphides with gallium sulphide, and aluminium sulphide are known to exist. While most of these glasses are stable with high glass transition and crystallization temperatures, the glasses based on aluminium sulphide are hygroscopic and are slowly destroyed by atmospheric moisture. The gallium sulphide-based glasses transmit very well into the infrared with a transmission cut-off at 10 μm. These glasses doped with neodymium also show good fluorescent properties.

Research in the oxides and oxysulphides of lanthanides (La–Nd) has identified them to form good homogeneous glasses with gallium sulphide [16–20]. Several other additions to gallium sulphide-based rare-earth glasses such as MnS, Ag_2S, have also been studied and the influence of these additions on the electrical and optical properties has been assessed as well [21]. Loireau-Lozac'h *et al.* [22] identified the glass-forming region in the La_2S_3–GeS_2–Ga_2S_3 system, while we have investigated the thermal and microstructural aspects of La_2S_3–GeS_2 glasses. In this review, salient features of glass formation, structure and properties of rare-earth-based chalcogenide glasses will be described with lanthanum sulphide, La_2S_3, being the rare-earth sulphide in most of the cases.

2.2 The gallium sulphide-rare-earth sulphide system

Gallium sulphide by itself is not known to be an easy glass former. Fast quenching has been reported to result in a disordered wurtzite-like compound and hence, melt quenching using rapid solidification processing could be a viable route to making gallium sulphide glasses, as demonstrated in the case of Sb_2S_3 [23]. While the formation of pure gallium sulphide glasses is difficult, additions of gallium sulphide in certain amounts to other sulphide compounds has been reported to result in glasses quite easily [18]. Extensive experiments carried out by French researchers [17, 18, 23–25] have shown that Ga_2S_3 forms glasses with a majority of sulphides from the lanthanide series with the exception of thulium, ytterbium and lutetium. In the case of europium (Eu), two glass-forming regions have been reported with the monosulphide of europium. The extent of glass formation of Ga_2S_3 with all the rare-earths is shown in Fig. 3. Lanthanum sulphide, La_2S_3 shows the largest glass-forming region in comparison with all the other rare-earth sulphides. The glass-formation domain for the glasses containing lanthanum sulphide is shown with respect to the phase diagram in Fig. 4. Loireau-Lozac'h *et al.* [22] synthesized several glasses by batching the stoichiometric glass compositions in a

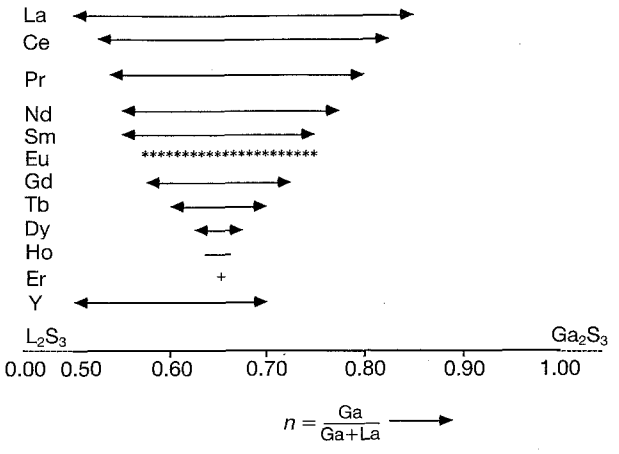

Figure 3 Extent of glass formation of Ga_2S_3 with rare-earth sulphides. (↔, ——, +) homogeneous glass; (∗) glass with crystals.

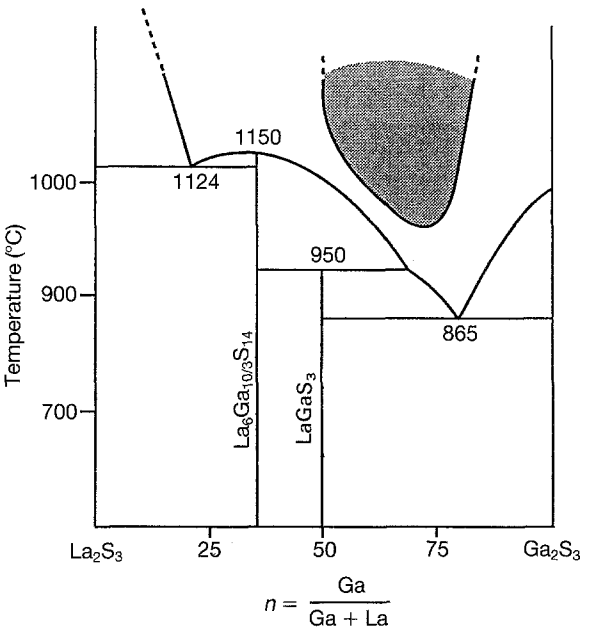

Figure 4 Glass-forming region in the Ga_2S_3–La_2S_3 system. Glass formation is seen in Ga_2S_3 rich compositions.

graphite crucible placed inside a fused silica tube. The tubes were sealed after evacuating to a pressure of 10^{-5} torr, heated to a temperature of 1200 °C and then subsequently quenched after a period of 2 h in water.

The glasses are pale yellow in colour and show a broad range of transparency from 0.5–10 μm as reported by Flahaut *et al.* [18]. They therefore make good mid-IR transmitting glasses similar to GeS_2. Flahaut *et al.* [18] studied glass formation of gallium sulphide with several rare-earth sulphides and measured the refractive indices of these glasses to be around 2.5 at 500 nm wavelength, depending on the quenching conditions and homogenization periods. They observed variation in the refractive index values with different sulphur contents in the glasses. These glasses doped with Nd^{3+} also show fluorescent properties. The laser cross-sections and radiative life times at 1077 nm are shown in Table IV for these glasses. Values for other oxide, oxysulphide, oxyhalides and halides are also included. The laser cross-sections are larger and the radiative lifetimes smaller than those reported for the oxide, oxyhalide and halide glasses. These properties, therefore, make these rare-earth glasses doped with Nd^{3+} good candidates for laser application [26].

Flahaut *et al.* [18] also studied the thermal stability of these glasses and observed that the Ga_2S_3-based rare-earth sulphide glasses show good stability and have high transition temperatures of about 620 °C. According to their findings, gallium sulphide seems to have very little effect on these glasses and the glasses tend to show a decreasing trend in the glass transition, (T_g), temperatures with increasing gallium sulphide contents. The crystallization temperatures, (T_c), of these glasses also show a similar behaviour to T_g with the observation of a single exothermic peak indicating the crystallization of a single phase.

Benazeth *et al.* [27] also recently studied the structure of these glasses using Raman spectroscopy (RS)

TABLE IV Laser cross-sections and radiative lifetimes at 1077 nm for oxide, halides and chalcogenide glasses

Glass	Wavelength, λ_p(nm)	Stimulated emission cross-section σ(pm^2)	Radiative lifetime, τ_R(μs)
Oxides			
Silicate	1057–1088	0.9–3.6	170–1090
Phosphate	1052–1057	2.0–4.8	280–530
Borate	1054–1062	1.51–1.69	270–450
Halides			
Fluoroberyllate	1046–1050	1.6–4.0	460–1030
Fluorozirconate	1049	2.9–3.0	430–450
Chloride	1062–1064	6.0–6.3	180–220
Oxyhalides			
Fluorophosphate	1049–1056	2.2–4.3	310–570
Chlorophosphate	1055	5.2–5.4	290–300
Rare-earth chalcogenides			
Ga_2S_3–La_2S_3	1075–1077	7.9	100
Al_2S_3–La_2S_3	1075–1077	8.2	100
Rare-earth oxysulphides			
Gd_2O_2S–Ga_2S_3	1075	4.2	92

and extended X-ray absorption fine structure (EXAFS). Their results show that the gallium ions in the glass exist as tetrahedral networks of GaS_4 and the Ga–S distances in the glasses are identical to those existing in the crystalline form of Ga_2S_3. However, there were some structural differences observed which can be seen in the Raman spectra collected on the glasses and the crystalline material shown in Fig. 5 [27]. The sharp peak at 233 cm^{-1} is characteristic of the stretching mode of GaS_4 tetrahedra and, while being present in the crystalline form of Ga_2S_3, is absent in the glasses. This has been interpreted in terms of structural modifications of the short-range periodicity around the gallium atoms, although there is no conclusive evidence. Results of the EXAFS analysis performed by them have shown the gallium and sulphur environments in the glasses to be similar to that seen in crystalline Ga_2S_3. The glasses seem to be comprised of tetrahedrally coordinated gallium atoms which form the glass-forming unit linked to each other at the corners. The lanthanum environment is also very similar to that present in the crystalline state of $La_6Ga_2Mn_2S_{14}$ but the La–S distances are reportedly more scattered, indicating significant distortion compared to the crystalline state. Based on the above facts reported by Benazeth *et al.* [27], they have suggested a possible structural model for these glasses. The gallium and sulphur environment in crystalline Ga_2S_3 predicts that two of the three sulphur (S_1 and S_2) atoms are linked to three gallium atoms and the third sulphur atom is linked to two gallium atoms. The bonds that link two of the three sulphur atoms to three gallium atoms consist of two covalent bonds and a third dative bond, while the third sulphur atom linked to two gallium atoms represents the bridging atom. Such a coordination for the sulphur atoms is not very typical for the sulphide glasses which is probably the reason for not easily obtaining pure Ga_2S_3 in the glassy state by melt quenching. However, the addition of La_2S_3 brings in an additional S^{2-} anion that results in modification of the dative bond of the trigonally coorindated sulphur atom. The dative bond is broken and then S^{2-} anion brought in by the modifying rare-earth sulphide helps in restoring and maintaining the tetrahedral environment of GaS_4 at the same time creating a negative site for the La^{3+} cation. A schematic representation of the structures described by Benazeth *et al.* [27] is shown in Fig. 6.

2.3. The aluminium sulphide–rare-earth sulphide system

Glass formation has been reported in the literature in Al_2S_3 containing varying amounts of the rare-earth sulphide. In these glasses also, aluminium sulphide contributes to glass formation and is, in fact, a better glass former than gallium sulphide. The glass-forming

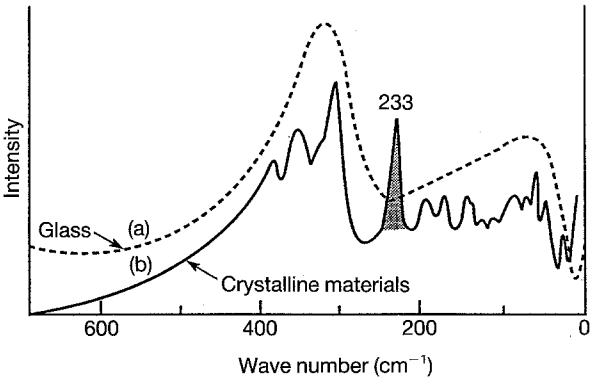

Figure 5 Raman spectra of amorphous and crystalline materials in the Ga–La–S system. Note the absence of the peak at 233 cm^{-1} in the glasses, corresponding to the stretching mode of GaS_4 tetrahedra. See the text for further details.

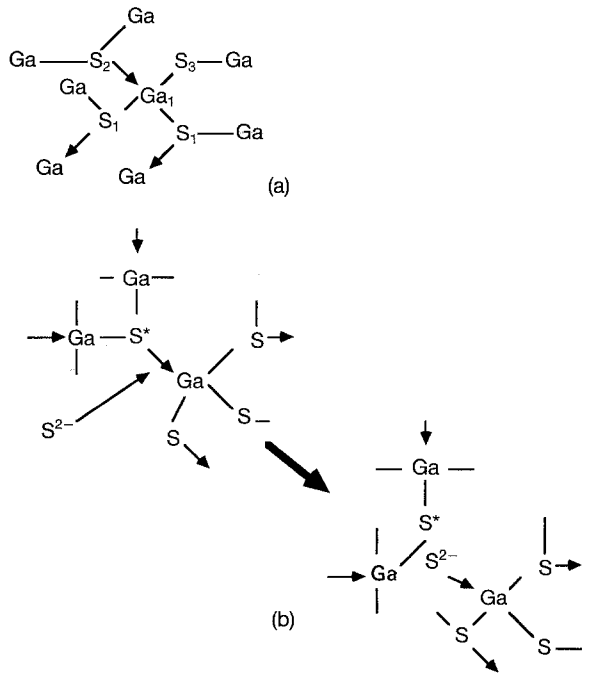

Figure 6 Schematic representation of the structure of glasses in the Ga_2S_3–La_2S_3 described by Benazeth *et al.* [27]. Note the difference in the environments of the three different sulphur atoms.

region has been reported to extend from 63–82 mol % Al_2S_3. Glasses in this system can also be obtained by fast cooling of the melts in vitreous carbon crucibles placed in SiO_2 tubes. The glasses are obtained by reacting lanthanum sulphide mixed with aluminium in an H_2S atmosphere for a period of 7 h in an induction furnace, to eliminate bubble formation and to ensure good homogeneity, after which the melts are cooled. Aluminium sulphide, Al_2S_3 forms glasses with most of the rare-earth sulphides with the exception of europium and terbium, the glass-forming domain again being the largest for La_2S_3. These glasses transmit well in the visible and in the infrared exhibiting a transmission cut-off at around 6 μm. The glasses also show good thermal stability with glass transition temperatures of 540 and 560 °C and crystallization temperatures of 660 and 680 °C for compositions correponding to 88 and 75 mol % Al_2S_3, respectively. The glasses are, however, not chemically stable and are easily attacked by water, limiting the use of these glasses for practical applications to a large extent [28].

2.4. The Eu–As–S ternary system

Several glasses in this ternary system have been reported in the literature [29] and the extent of glass formation is shown in Fig. 7. Glasses in this system can be prepared by mixing EuS, As_2S_3 and elemental sulphur in evacuated fused silica tubes which are heated in steps gradually to 800 °C and then quenched in water. The EuS used can be prepared by the gas-phase reaction to H_2S with Eu_2O_3 at 1200 °C, while the As_2S_3 is used typically after distillation at 650 °C to remove any oxygen impurities in the sulphide. These glasses show lower thermal stability and crystallize in the temperature range of 300–400 °C, with glass transition temperatures being in the range of 200–250 °C. While thermal stability of these glasses is lower than the other rare-earth glasses, they exhibit good transmission in the infrared, with the transmission cut-off being ≈ 10 μm, although large absorption bands corresponding to the stretching frequencies of S–S and S–H bonds are seen in the transmission spectra of these glasses. Barnier *et al.* [29] have studied the structure of these glasses using Raman and infrared spectroscopy, which shows that europium in these glasses exists in the divalent state, contrary to the trivalent state known to exist according to the phase diagram.

2.5. The germanium sulphide–lanthanum sulphide system

Glasses in this system have been synthesized by mixing stoichiometric amounts of GeS_2 with La_2S_3. The glass-forming domain for these glasses extend from 60–100 mol% GeS_2 and is shown with respect to the GeS_2–Ga_2S_3–La_2S_3 ternary system in Fig. 8 [30, 31]. There is no equilibrium phase diagram available for this system, although Sarkisov *et al.* [32] made attempts to study compound formation in this system using differential thermal analysis (DTA). They identified two congruently melting compounds, $La_2Ge_2S_7$ and La_2GeS_5 and the presence of three eutectics at 92.5, 60 and 43 mol % GeS_2, respectively. The schematic phase diagram based on their DTA analysis is shown in Fig. 9. The phase diagram shows one deep eutectic at 92.5 mol % GeS_2 while the eutectics at 60 and 43 mol % are more or less shallow. In this system, similar to glasses containing Ga_2S_3, GeS_2 acts as a flux and promotes glass formation to occur in compositions rich in GeS_2.

We have synthesized germanium sulphide–lanthanum sulphide glasses using standard chalcogenide glass-forming techniques [6, 30, 31, 33]. Germanium sulphide, GeS_2 (99.99% purity metals basis; Alfa Chemicals, Johnson Matthey, Alfa Products, P.O.Box 8247, Ward Hill, MA) and the tetragonal (β) form of La_2S_3 (99.9% purity; Cerac Chemicals, Cerac Inc., P.O. Box 1178, Milwaukee, WI) were commercially obtained and used for glass making. The glasses were made by weighing stoichiometric amounts corres-

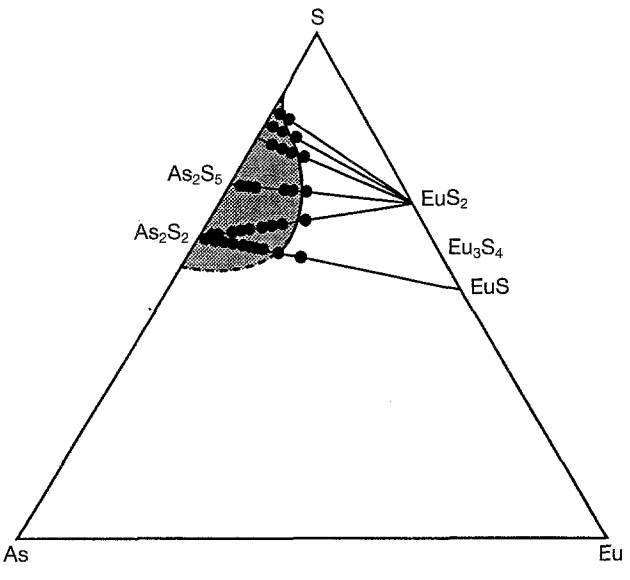

Figure 7 Extent of glass formation in the Eu–As–S system.

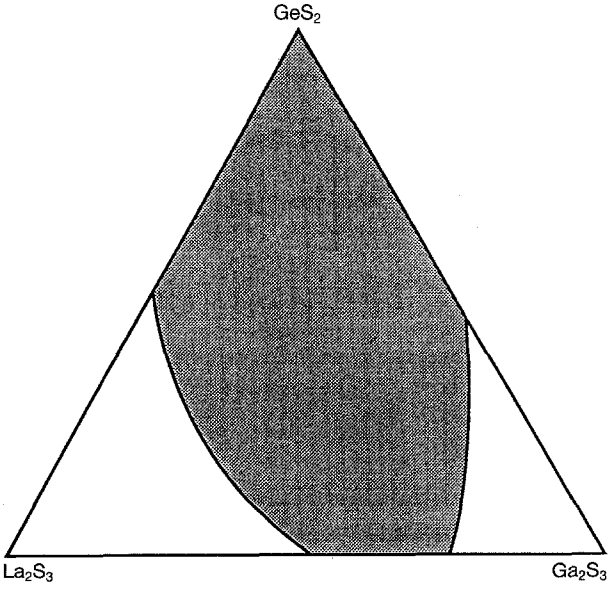

Figure 8 Extent of glass formation in the ternary GeS_2–Ga_2S_3–La_2S_3 system.

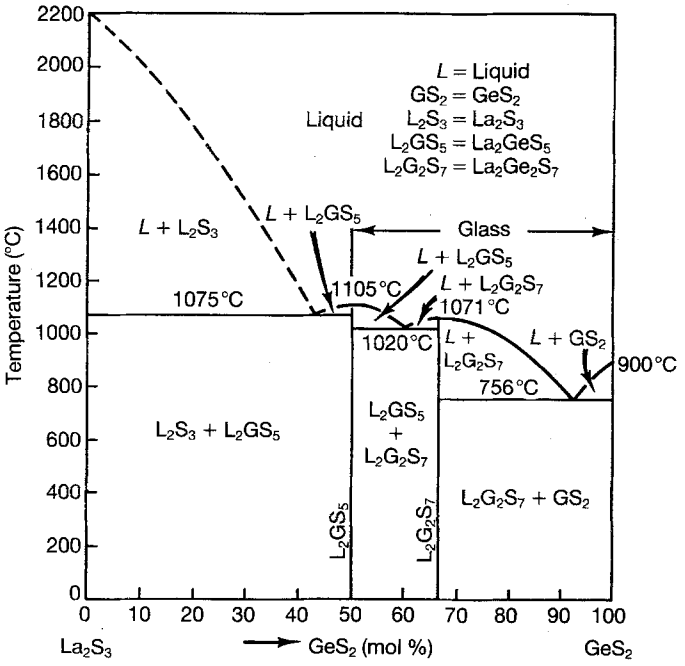

Figure 9 Schematic phase diagram in the GeS_2–La_2S_3 system based on the data of Sarkisov *et al.* [32].

ponding to respective glass compositions in a dry box and batching them into carbon-coated fused silica tubes. The tubes were then evacuated to a pressure of $\approx 10^{-5}$ torr and sealed. The sealed tubes were subsequently heated to a temperature of 1175 °C in an electrically heated box furnace and the melts homogenized for a period of 24 h. Compositions rich in GeS_2 were prepared by initially heating the tubes to a temperature of 1000 °C and holding them for 10 h after which they were homogenized at 1175 °C for 14 h.

The GeS_2 glasses containing La_2S_3 are optically dense and their colour varies from ruby red to brown. Compositions richer in GeS_2 tend to be dark brown. These glasses show some interesting features with increasing concentrations of germanium sulphide when observed under the transmission (TEM) and scanning electron microscopes (SEM) [30, 31]. Fig. 10 shows the bright-field image picture of a 60 mol % La_2S_3. The glasses are homogeneous and show no presence of any secondary phases. The diffraction pattern shown in the inset confirms the amorphous nature of the glass. On the other hand, with increasing GeS_2 concentrations in these glasses there is evidence of phase-separation. Fig. 11 shows the microstructure corresponding to the primary phase separation in these glasses. The phase-separated droplets are in the range 88 nm (largest droplet) to 6 nm (smallest droplet) uniformly distributed as indicated by the micrographs. Similar phase-separation at the molecular level has been observed in the literature in several sulphide glasses containing GeS_2 and Na_2S and also in GeS_2 glasses containing Li_2S [34]. In all these cases, phase-separation has been reported in the GeS_2-rich compositions such as $90GeS_2$–$10Li_2S$ and $80GeS_2$–$20Na_2S$ similar to the rare-earth sulphides. The excess sulphur molecules (in the Ge–S phase) separate out and in fact are visible as etch pits when the sulphur chains are dissolved in CS_2, the sizes of the

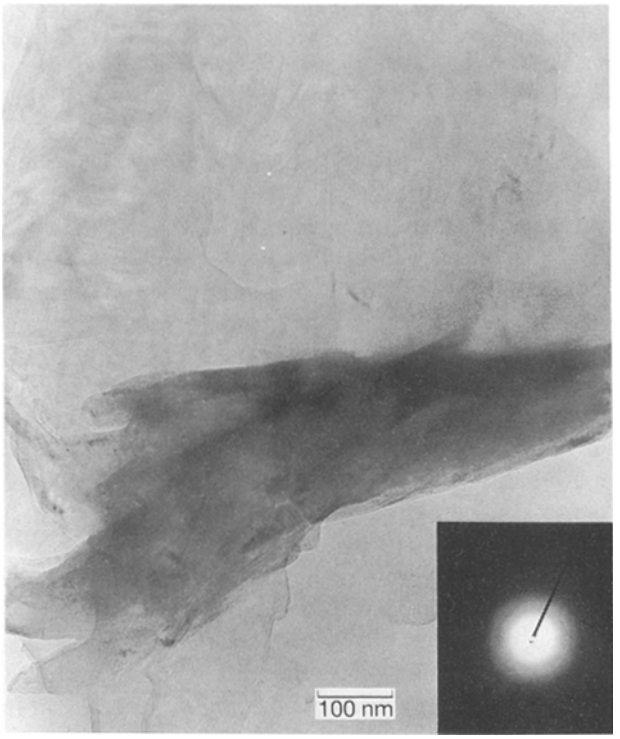

Figure 10 Transmission electron bright-field image of glass containing 60 mol % GeS_2–40 mol % La_2S_3. The glasses are homogeneous and show no presence of any secondary phases.

phase-separated droplets being of the order of 0.5–2 μm.

These experiments and previous results in the literature on sulphide glasses containing germanium indicate that the phase-separation seen in the system is also probably occuring because of excess GeS_2. The small size range of the phase-separated droplets prevents the use of conventional microscopic chemical analysis techniques such as EDX to estimate the composition of the phase-separated droplets because of the substantial penetration depths and large inter-

Figure 11 Transmission electron bright-field image showing primary phase-separation in glasses containing 92.5 mol % GeS_2. Note the presence of glass droplets in the size range of 6–88 nm distributed in the glass matrix.

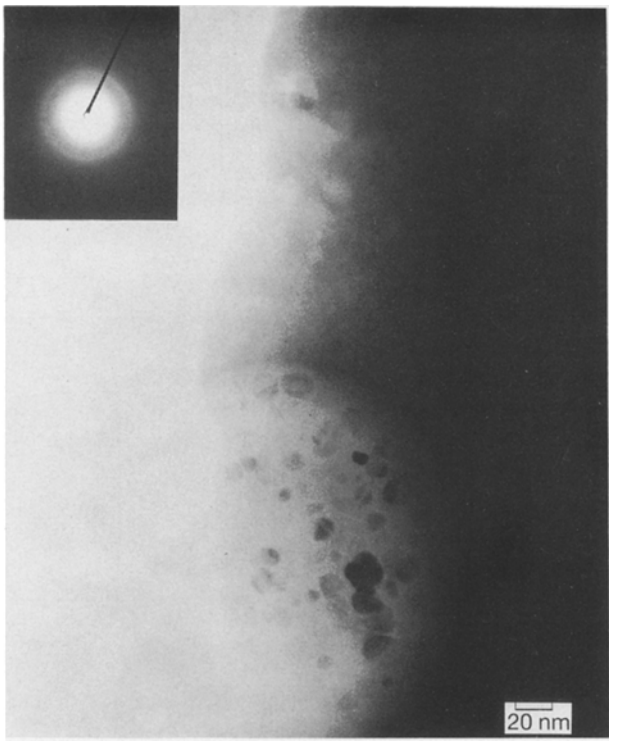

Figure 12 Transmission electron bright-field image of glasses containing 92.5 mol % GeS_2 showing the formation of secondary phase-separated droplets in the range 3–13 nm dispersed in a 200 nm primary droplet. The inset shows the amorphous pattern corresponding to the glass matrix.

action volume of the electron beam. An additional interesting feature exhibited by these glasses is the presence of secondary phase separation, as shown in Fig. 12. The figure shows a primary droplet $\approx$ 200 nm in size in which are embedded the secondary phase-separated droplets ranging from 3–13 nm in size. Some of the secondary phase-separated droplets are, in fact, crystalline with visible lattice fringes. Secondary phase-separation has been known to occur in oxide systems and recently, some reports on primary and secondary phase-separation in fluoride systems can also be found. Such an occurrence in these rare-earth sulphides is not very common.

There have been no detailed studies regarding the phase-separation kinetics and hence, based on experimental evidence, only some speculations have been made. The primary phase-separation occurs probably because of the presence of an immiscibility region in the GaS_2–La_2S_3 system which results in a sulphide-rich $Ge_{1-x}S_x$ composition (where x may be a variable) separating from the glass matrix during air cooling. Upon further cooling, sulphur droplets could be phase-separating out in the primary droplet of $Ge_{1-x}S_x$ glass, forming the secondary droplets. There is no exact phase diagram showing the miscibility gaps in this system which could be used to extract information about the mechanism of phase-separation and consequently, there is a need for further research in this direction.

We have assessed the thermal stability of these glasses using differential thermal analysis (DTA) conducted on crushed samples after purging the system with inert helium gas. The glasses in this system exhibit glass transition temperatures, T_g of approximately 420–510 °C, depending on the amounts of GeS_2 in the glasses. The crystallization temperatures, T_c also show similar variation from 559–790 °C. Glass transition and crystallization temperatures show a decreasing trend with increasing germanium sulphide contents consistent with the low transition temperatures of germanium sulphide. Glasses containing 60 mol % GeS_2 crystallize to form single-phase β-La_2S_3. This shows that the GeS_2 tends to remain in the amorphous state and only lanthanum sulphide crystallizes out of the glass. Both GeS_2 and polycrystalline β-La_2S_3 are known to transmit up to 10 μm, but the β form of lanthanum sulphide possesses higher mechanical strength, and is also more refractory with a lower thermal expansion coefficient. Hence, in combination with GeS_2 there is potential for this glass composition to be used as a glass ceramic to strengthen the GeS_2 glass matrix, particularly for optical fibre application in mid-infrared regions.

So far in the discussion, pure sulphide glasses with rare-earth cations added as sulphides have been considered. However, glass formation has also been observed with the rare-earth cation being introduced in the oxide and oxysulphide forms resulting in the formation of oxysulphide glasses. The following section deals with the formation and characteristics of these glasses.

2.6. Rare-earth oxide and oxysulphide systems

Research in this category of glasses has been focused mainly on the oxide and oxysulphides of lanthanum

with addition of varying proportions of gallium sulphide, although for the oxysulphide glasses, additions of other rare-earth sulphides have also been investigated. There has been extensive research conducted by Flahaut and co-workers [18–20] on glass formation in these systems in addition to their work on Ga_2S_3 and Al_2S_3-based rare-earth glasses discussed above. An extended region of glass formation has been observed in the La_2S_3–La_2O_3–Ga_2S_3 system, which is shown in Fig. 13. The glass-formation region is extended towards the lanthanum-rich region, probably because of the existence of a ternary eutectic. The quasi-binary section of the ternary system comprising La_2O_2S and Ga_2S_3 has been investigated with regards to glass formation by Flahaut *et al.* [18], and the glass-forming region is shown in Fig. 14. Glass-forming regions in this phase diagram also correspond to regions in the vicinity of the eutectic composition, similar to the case of gallium-based rare-earth sulphide glasses. However, the glass-formation region does not include the eutectic composition, which shows that the glass formation is governed not only by the presence of a eutectic but is also dependent on the chemical composition and structure. As indicated in Fig. 14, glasses can be obtained in the composition range roughly extending from 60–80 mol % Ga_2S_3. Similar glass-forming domains exist for glasses containing oxysulphides of cerium, praseodymium and neodymium [18].

The glasses are typically obtained by quenching following the conventional technique described above, but the quenching temperatures are limited to 1100 °C due to the formation of SO_2 which can cause explosion of the fused silica tubes. The same restriction has been observed in the case of the glasses containing La_2O_3 and Ga_2S_3. The glasses are transparent and exhibit several colours; yellow with lanthanum, red with cerium, and green with praseodymium and neodymium. They are optically dense with refractive indices of 2.30–2.50 in the visible range of 400–700 nm, the values of 2.3 and 2.5 being recorded at 700 and 400 nm, respectively [20]. These glasses show much better chemical stability and are more resistant to atmospheric moisture attack in comparison to the corresponding sulphides. They also exhibit reasonably good thermal stability, similar to the gallium sulphide-based rare-earth glasses and show glass transition temperatures around 600 °C which show a decreasing trend with increasing Ga_2S_3 contents.

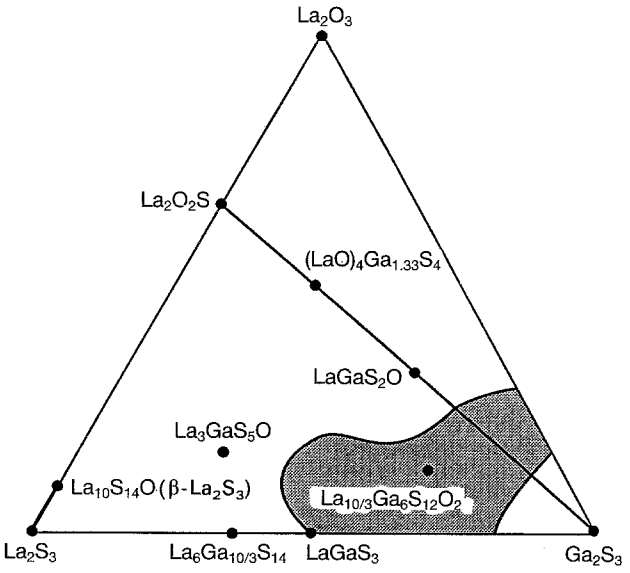

Figure 13 Extended glass forming region in the ternary oxide sulphide system of La_2S_3–La_2O_3–Ga_2S_3 indicated by the shaded region.

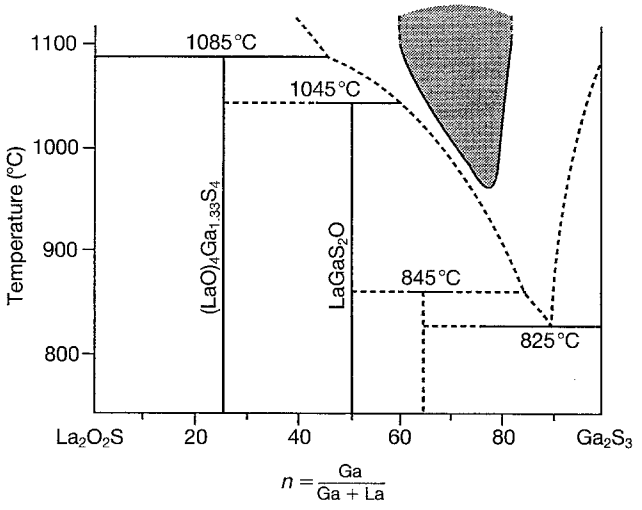

Figure 14 Glass-forming domain (shaded area) in the La_2O_2S–Ga_2S_3 pseudo-binary system. Glasses are formed in the compositions containing 60–80 mol % Ga_2S_3.

2.7. Novel glasses in the rare-earth sulphide systems

The rare-earth sulphide glasses form a new class within the chalcogenide system and many of these glasses show some very interesting properties. Table V summaries the properties of several rare-earth sulphide glasses most of which have been discussed above. The excellent far-IR transmitting characteristics of the rare-earth sulphides coupled with the glass-forming ability of chalcogenides make these glasses very good candidate far-IR transmitting materials. The glasses are also more thermally stable in comparison to other chalcogenide glasses, with glass transition temperatures greater than 500 °C. The crystallization of the mechanically stronger rare-earth sulphide phase from the glasses in some cases also shows potential for using them as glass ceramics for optical applications. Glasses doped with neodymium show good fluorescent properties with large stimulated emission cross-sections and reduced radiative lifetimes. There has also been some recent studies on the addition of dysprosium and holmium on the lasing properties of glasses containing germanium and arsenic sulphides [35]. While glasses have been studied for their microstructure and optical and electrical properties, the need for mechanically and thermally strong materials with good optical transmission in airborne applications has led researchers to study crystalline chalcogenide ceramics.

TABLE V Optical and thermal properties of rare-earth-based glasses

Rare-earth glasses	Thermal properties		Optical properties	
	T_g(°C)	T_c(°C)	Refractive index, n at λ = 400–700 nm	Transmission range (μm)
Ga_2S_3–La_2S_3	≈ 620	–	2.4–2.8	0.5–10
GaS_2–La_2S_3	≈ 420–510	559–790	–	–
La_2S_3–Ga_2S_3–Ag_2S	410–480	525–585	–	–
Ga_2S_3–La_2S_3–MnS	550–590	≈ 675	–	–
Eu–As–S	185–226	336–397	–	0.5–10
Al_2S_3–La_2S_3	540–560	660–680	–	0.5–6.0
Ga_2S_3–La_2O_2S–MnS	≈ 590–610	640–720	–	–
Ga_2S_3–La_2O_2S	590–610	640–810	2.3–2.54	0.4–5.0
Ga_2S_3–La_2O_3–MnS	485–535	585–695	–	–
Ga_2S_3–La_2O_3	560	–	–	–

3. Optical sulphide ceramics

The rare-earth sulphide glasses have emerged as a new class of amorphous materials in the chalcogenide system. They display several unique properties that increases the potential applications of these materials, thereby widening the scope of the chalcogenides. The long wavelength transmission characteristics exhibited by these materials promoted research into using these materials for application as windows in heat-seeking missiles. The detection of infrared radiation for sensing low-temperature objects forms the basis for far-IR optical windows. The spectral emittance curves from a black body follow the familiar Wien's displacement law ($\lambda_m T = 2.898 \times 10^{-3}$ m − K) where λ_m is the wavelength at which the emissive power is the maximum. Based on this equation, therefore, to detect objects at room temperature, the 8–14 μm IR window is most suitable [36]. The good optical properties of these sulphides has prompted major research to be conducted in the fabrication of materials that transmit into the IR wavelength region. These materials will therefore continue to play a major role in the development of future target-acquisition and weapon-aiming devices, surveillance equipment, alerting devices and missile-homing seekers [37]. While the transmission characteristics of sulphide glasses are favourable for their use in long wavelength applications, their low softening points and high thermal expansion coefficients preclude them from use in optical window applications. There was, therefore, a mounting interest to look for new crystalline materials that could be suitable as optical windows. The early part of the last decade witnessed intense research that was conducted at several universities and the Naval Research Laboratory, for identifying materials that could be used for these applications.

The window materials used in the equipments deployed on aircraft and guided weapons are subjected to harsh environmental conditions, in particular aerodynamic heating, thermal shock and rain erosion. Thus, the thermal and mechanical properties of the window material must be near optimum if the windows are to survive these environmental conditions. Far-infrared windows should therefore meet the following requirements for optimum thermal, mechanical and optical properties, namely, high melting point, low coefficient of thermal expansion, large band gap, good transmission into the far-infrared (8–14 μm), high hardness, and good strength.

These requirements make the choice of materials available very limited. Semiconductors (silicon and gemanium) exhibit good transmission in the far-infrared and are also adequately strong, however, free electron absorption at 100 °C makes these materials opaque and hence limits their use. From optical transmission, thermal and mechanical considerations, ZnS is the most suitable window material for use in the particular wavelength of interest for airborne window applications. On the other hand, its low hardness and poor resistance to severe rain erosion conditions does not make it the most suitable material. Table VI lists some of the infrared transmitting materials [38]. Oxides possess the required mechanical properties because of the strong M–O bond but display limited IR transmission due to the high fundamental vibration frequencies (especially when M is a light element) resulting in short wavelength cut-offs rendering them opaque in the 8–14 μm range. A massive anion is therefore desirable to promote IR transmission making the search for non-oxide ceramics inevitable [36, 38]. Table VII lists the currently interesting IR materials.

In general, materials with strong chemical bonds exhibit good thermo-mechanical properties but poor infrared transmission, and materials that transmit very well possess weaker chemical bonds and poor thermal and mechanical properties. Hence, a compromise is necessary [39, 40]. A materials study to find an advanced optical window material was conducted with the focus on polycrystalline materials that exhibit the cubic crystalline structure. The cubic and spinel structures generally exhibit useful infrared transmission. In addition, the optically isotropic nature of the cubic structure allows window parts to be made from polycrystalline materials without much loss due to scatter. The search to find an advanced material better than ZnS for the 8–14 μm airborne application led to the understanding that the alkaline earth–rare-earth ternary compounds of the formula AB_2S_4 (particularly $CaLa_2S_4$) would be ideal candidate materials for far-IR applications [37]. Preliminary studies had indicated that materials in this group displayed good

TABLE VI Potential infrared window materials and their properties

Material	Transmission range (μm)	Thermal expansion ($10^{-6}\,°C^{-1}$)	Melting point (°C)	Hardness (kg mm^{-2})	Young's modulus (GPa)
ZnS	0.5–12	7.5	1700	250	75
GeS	1–10	20	200[a]	120	–
$CaLa_2S_4$	0.5–14	13	1800	600	96
As_2S_3	0.6–10	20	200[a]	120	–
La_2S_3–Ga_2S_3	0.5–10	–	620[a]	–	–
La_2O_2S–Ga_2S_3	–	–	600[a]	–	–
La_2S_3	0.5–14	10	2100	670	–
GeS_2	1–10	20	250[a]	130	–
$CaNd_2S_4$	0.5–14	13	1830	650	–
Ge	2–16	6.0	936	700	100
Si	1–10	4.0	1420	1150	190
GaAs	1–16	5.7	1240	750	85
ZnSe	0.6–14	7.6	1520	100	60
Diamond	> 4.5	1.5	4000 K at 130 kb	9000	–

[a]Glass transition, T_g.

TABLE VII Properties and preparation techniques of some current and future IR window and dome materials

Material	Transmission range (μm)	Preparation technique	Level of usefulness
ThO_2–ZrO_2	0.5–5	Hot-pressed	Future
ZrO_2–Y_2O_3	0.5–5	Single crystal with precipitates	Near-future
MgF_2	0.3–5	Hot-pressed	Current
$MgAl_2O_4$ (spinel)	0.3–5	Hot-pressed	Near-future
Al_2O_3 (sapphire)	0.3–5	Flame fusion	Current
SiC	0.3–6	CVD	Future
Al_2O_3–SiO_2 or GeO_2	0.3–5	Hot-pressed	Future
AlN	0.3–5	Hot-pressed	Future
Si_3N_4	0.6–5	CVD	Near-future
ZnS/ZnSe (sandwich)	1–12	CVD	Current
$CaLa_2S_4$, $BaLa_2S_4$, $CaNd_2S_4$, $SrSm_2S_4$, etc. (ternary sulphides)	0.5–14	Hot-pressed HIP	Future
La_2S_3 (cubic)	0.5–14	Hot-pressed	Future

transmission up to 14 μm, low free electron absorption, high melting point, high hardness (600 kg mm^{-2} for $CaLa_2S_4$) and also possessed the cubic symmetry (Th_3P_4 type) [41–43]. The large coefficient of thermal expansion of $CaLa_2S_4$ ($14.7 \times 10^{-6}\,°C^{-1}$) makes this material inferior compared to ZnS, although its hardness and Young's modulus are higher than those of ZnS, suggesting a better performance in rain erosion environments (see Table VI).

3.1. Structure and processing of calcium lanthanum sulphide

The structure of $CaLa_2S_4$ bears a strong resemblance to the structure of cubic La_2S_3. Zachariasen originally characterized some of the rare-earth sesquisulphides as having the Th_3P_4 structure, particularly Ce_2S_3 which is isostructural with La_2S_3 [44, 45]. The cubic phase of La_2S_3, also represented as the γ-phase is a defect Th_3P_4 structure. Zachariasen identified the space group of this phase to be $I\bar{4}3d$ which was also verified subsequently by the authors using the emerging technique of convergent beam electron diffraction. The unit cell consists of 16 sulphur atoms and $10\frac{2}{3}$ lanthanum atoms, with metal vacancies being randomly arranged such that every ninth position is vacant [44]. Flahaut and other workers [45–48] performed much of the early work on this system. They indicated that by filling up the vacancies a range of compositions spanning the complete solid-solution region could be obtained from R_2X_3 to R_3X_4. In the case of $CaLa_2S_4$, the study basically originated from the processing difficulties that existed for synthesizing the cubic phase of La_2S_3 which forms at temperatures in excess of 1500 °C. The probability for the Th_3P_4 structure to exist for any phase would be ideal if the cation to anion ratio approached 3:4. It was found by researchers [48] that small amounts of large divalent cations stabilize the Th_3P_4 structure at much lower temperatures. There is, therefore, a continuous and homogeneous range of stoichiometries for the ternary $Ca_{1-x}La_2S_{4-x}$, for $x = 1\text{-}0$ [47]. The calcium and lanthanum atoms are distributed over the twelve sites of point set corresponding to site symmetry 4, while the sulphur atoms fully occupy the sixteen sites of point site corresponding to site symmetry 3.

Saunders *et al.* [49] studied the formation and structure of $CaLa_2S_4$. They observed that there is a region in the triangular composition field in the phase

diagram wherein single phase $CaLa_2S_4$ forms. Their study indicates that $CaLa_2S_4$ forms a complete series of solid solutions with La_2S_3 and La_3S_4 as shown in Fig. 15, with the heavy line corresponding to fully sulphurized compositions. Based on their study, they indicated a generalized chemical formula for calcium lanthanum sulphide to be $Ca_{1-x}La(III)_{2+(6/9)x-(8/9)y}La(II)_{(8/9)y}S_{4-(4/9)y}[]_{(4/9)y}$ where [ ] represents a sulphur vacancy. They used the parameters $0 \leqslant x, y \leqslant 1$ to describe all the compositions in the single-phase field where x and y address all the cation and anion stoichiometries. They also used this information to study the effect of variation of the La:Ca ratio on the optical quality of the ceramic.

This material possesses the defect cubic Th_3P_4 structure and shows a potential IR cut-off at 14 μm with a band gap of 2.7 eV as shown in Table V. Calcium lanthanum sulphide, $CaLa_2S_4$ exists as a light yellow powder and two processing methods have been generally followed by researchers to synthesize this material. The cubic γ-phase of the rare-earth sulphides is the one that is desired for transmission and the introduction of the bigger divalent alkaline earth cation tends to stabilize this cubic structure. Raytheon [50] developed a process for fabrication of this material which comprised three steps. A solution containing the respective nitrates was converted to the corresponding carbonates by reacting with ammonium carbonate. The powder was then dried at 40 °C for 48 h after which it was heated at 1000 °C for 20 h under 1 atm flowing H_2S to give the light yellow powder of $CaLa_2S_4$. This powder was mixed with several binders such as polyvinylpyrrolidone, spray dried and isostatically compressed to give a green pellet. The green compact was then hot isostatically pressed (HIP) under argon gas after being pre-sintered in flowing H_2S for 10 h at 1050 °C to 1150 °C. The final HIP treatment resulted in ceramics with essentially theoretical density [49–52]. The other process was developed by Chess *et al.* [53] which consisted of obtaining oxide powders of calcium and lanthanum at 1000 °C using the evaporative decomposition of solutions (EDS) method. The method involved decomposition of a solution of nitrates of calcium and lanthanum. The resulting oxide powders were then converted to the sulphides by reacting with hydrogen sulphide at 1000–1350 °C. The sulphide powders were then hot pressed [53–55]. The characteristics of the precursors obtained using the EDS method are shown in Table VIII.

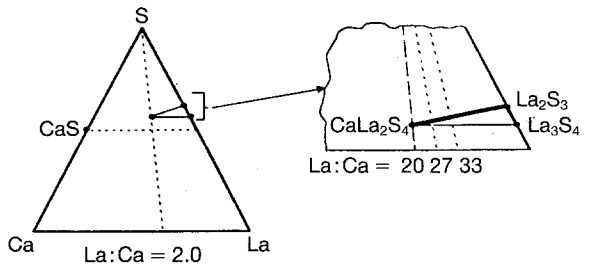

Figure 15 Ternary compositional diagram in the Ca–La–S system showing the $CaLa_2S_4$, La_2S_3 and La_3S_4 phase fields [49].

TABLE VIII Characteristics of precursors for calcium lanthanum sulphide prepared using the EDS method

Sample	Surface area (m^2/g^{-1})	Particle size	
		Measured (μm)	Calculated (μm)
Ternary sulphide prepared by dry firing	–	15	–
EDS oxide precursor (from 0.30 M solution)	10.8	5.5	3.1
EDS oxide precursor (from 0.15 M solution)	14.5	3.0	2.5
Ternary sulphide prepared from EDS oxide precursor	9.4	3.9	–

Savage *et al.* [56] incorporated the EDS method with various other methods to first obtain the fine-grained oxide powder that was subsequently heat treated in H_2S to obtain the desired sulphide. One of the methods consisted of using mixed nitrate solutions which were evaporated to a syrup in platinum and then fired to an oxide cake at 900 °C in air for 24 h. The resulting powder was then crushed and refired at 900 °C in air to form a white powder which was then subsequently converted to a sulphide by firing in H_2S/N_2 for 24 h at 1150–1350 °C. In another method they followed a rapid decomposition of solutions of mixed nitrates in air at 1000 °C with subsequent sulphidization [57, 58]. They also processed various compositions in the $CaLa_2S_4$–La_2S_3 phase diagram in an attempt to optimize the material chemistry to obtain useful physical and optical properties. Beswick *et al.* [58], on the other hand, in addition to the routes described above, used the oxalate route to prepare fine oxalate powders of calcium and lanthanum. The oxalates were precipitated from the nitrate solutions and the resulting precipitate filtered and dried. The dried precipitate was then converted to the sulphide by heat treatment in H_2S at 960 °C. They also utilized a sol-precipitation technique to obtain spherical oxide precursor particles that were converted to the sulphide by H_2S treatment. The characteristics of the powders obtained following their route is shown in Table IX, and the corresponding transmission spectra of the densified ceramic [obtained following some of the above routes], are shown in Fig. 16.

Gentilman *et al.* [59] also studied these compositions and analysed their mechanical and optical properties. They prepared powders using the EDS method and then densified the powders following the sinter /HIP technique as outlined by Raytheon. The transmission of these composition in comparison to ZnS is shown in Figs 17 and 18. From the figures it can be seen that increasing the fraction of La_2S_3 does not affect the transmission, suggesting that the cubic phase of La_2S_3 would be a potential candidate for far-IR transmission. However, the EDS precursor for lanthanum sulphide did not result in the formation of the cubic phase at lower temperatures. A comparison of some of the physical properties of $CaLa_2S_4$ and ZnS is given in Table X [56]. A comprehensive report on the fabrication of this material can be found in a publi-

TABLE IX Characteristics of calcium lanthanum sulphide powder prepared via different routes

Synthesis route[a]	Sulphidizing temperature (°C)	Product appearance	Phase composition	Particle size (μm)	Specific surface area (m^2g^{-1})	Oxygen content (p.p.m × wt)
A	1350	Biscuit	$CaLa_2S_4$	10	< 0.1	1.5×10^2
B	900	Soft powder	$CaLa_2S_4$ + trace CaS	≈ 1	nd	nd
C	900	Soft powder	$CaLa_2S_4$ + trace CaS	0.5–2	0.83	2×10^3
D	960	Fine powder	$CaLa_2S_4$ + trace CaS	0.5–2	nd	3×10^3
E	950	Fine powder	$CaLa_2S_4$	0.5–2	0.83	2.9×10^3
F	1050	Soft sintered block	$CaLa_2S_4$ + CaS	2 to 10	0.35	nd

[a]A Evaporation of mixed nitrates to a syrup and heated in air to 900 °C, powder crushed and refired to 900 °C for 15 h and then sulphidized for 24 h at 1150–1350 °C.
B Rapid decomposition of solution of mixed nitrates at 1000 °C in air. The oxide is then converted to the sulphide by sulphidization between 900 and 1100 °C.
C Evaporative decomposition of solutions (EDS) of a mixed nitrate solution in a furnace at 1000 °C in air to form a fine powder. The fine powder is then converted to the sulphide by sulphidization at 900 °C in hydrogen sulphide.
D Oxalates of lanthanum and calcium formed from the nitrates. The oxalates are then converted to the oxide by heating in air and then transformed to the sulphide at 960 °C.
E An organic acid is added to the mixed nitrate solution and the solution is converted to a voluminous foam by rotary vacuum evaporation. The precursor is converted to the oxide by firing in air and then converted to sulphide by heating in H_2S/N_2 at 950 °C.
F Sol–gel route if used to form the oxide precursor which is converted to the sulphide by heating in H_2S at 1050 °C.

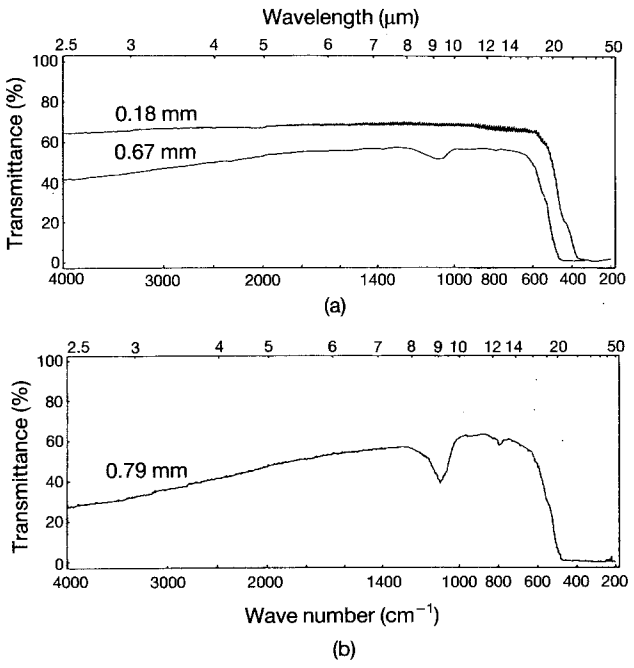

Figure 16 Infrared transmission spectra of sintered and hot isostatically pressed (HIP) $CaLa_2S_4$ ceramics processed from powders prepared using (a) rapid decomposition and (b) the rotary vacuum evaporation technique [57, 58].

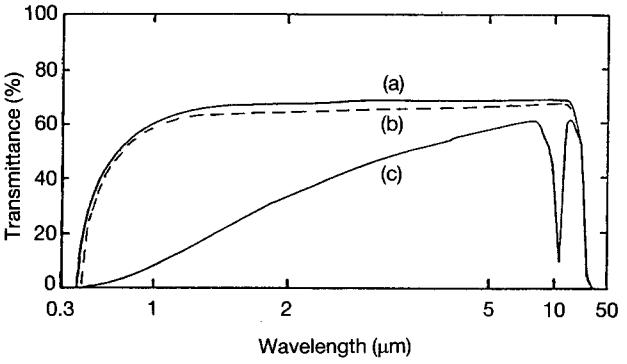

Figure 17 Variation of transmission in CaS–La_2S_3 with increasing amounts of La_2S_3. (a) Transmittance of sample 1.16 mm thick containing 45 mol % CaS and 55 mol % La_2S_3. (b) Transmittance of sample 1.0 mm thick containing 10 mol % CaS and 90 mol % La_2S_3. (c) Transmittance of $CaLa_2S_4$ 0.71 mm thick [59].

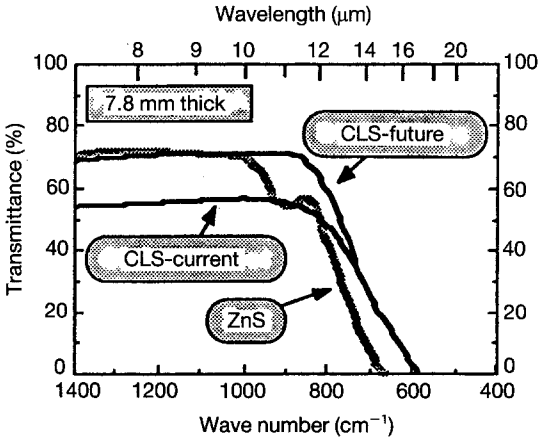

Figure 18 Comparison of the in-line transmittances of $CaLa_2S_4$ (current and future) and ZnS (7.8 mm thick) [59].

cation released by the Naval Weapons Center [60]. In this report the processing and evolution of state-of-the-art $CaLa_2S_4$ dome material corresponding to the stoichiometry of La_2S_3:CaS = 90:10 has been described. The report essentially summarizes the various techniques described above. Figs 19 and 20 show the flow sheets for the powder synthesis and processing of state-of-the-art $CaLa_2S_4$ [49, 60]. The optical, mechanical and thermal properties of the ceramic are compared to ZnS in Table XI. The thermal expansion coefficient is $14.7 \times 10^{-6}\,°C^{-1}$, which is about twice that of ZnS. The thermal conductivity is 1.7 $W\,m^{-1}K^{-1}$ which is one-tenth that of ZnS. Measurements of flexural strengths show that the ratio of strengths for $CaLa_2S_4$ to ZnS is about 80% which show that the ternary sulphide does not possess better mechanical

TABLE X Some physical properties of zinc sulphide and calcium lanthanum sulphide at the present state of development [56]

Property	Calcium lanthanum sulphide	Zinc sulphide
Flexural strength (MPa)	106	103
Young's modulus (GPa)	96	75
Poisson's ratio	0.26	0.27
Knoop hardness (GPa)	5.59	2.45
Thermal expansion ($10^{-6}\,°C^{-1}$)	14.7	7.4
Thermal conductivity at 25 °C (Cal $cm^{-1}s^{-1}\,°C^{-1}$)	0.006	0.041

TABLE XI Comparative properties of CLS (La:Ca = 2.7) and Raytran Zns (Standard Grade)

Property	CLS	ZnS
Optical		
Absorption coeff. (cm^{-1})		
10.6 (μm) (calorimetric)	0.12	0.3
Long wavelength cutoff[a] (μm)	11.5	10
Mechanical		
Hardness, knoop (kg mm^{-2})	570	250
Flexural strength (p.s.i.)[b]	7240	9300
Flexural strength (p.s.i.)[c]	12515	15128
Young's modulus (10^6p.s.i.)	13.9	10.8
Grain size (μm)	50	2
Impact damage threshold (1 damage site per 100 impacts 2 mm water drops)		
Bare (ms^{-1})	110–225	110
Yttria-coated (ms^{-1})	180	120
Thermal		
Expansion ($10^{-6}\,°C^{-1}$) (20–400 °C)	14.7	7.4
Melting point (°C)	1810	1830
Specific heat ($Jg^{-1}°C^{-1}$)	–	0.468
Conductivity ($Wm^{-1}K^{-1}$) (20 °C)	1.7	17.2
Density (g cm^{-3})	4.61	4.08
Thermal shock resistance ($Wm^{-1}s^{-1}$)	83.6	2340.8

[a] Corresponds to a 2 % drop in transmittance for a piece 7.8 mm thick.
[b] Measured on bars 0.250 in. × 0.500 in. × 4.00 in.; four point bend.
[c] Measured on discs 0.100 in. thick with a diameter of 0.875 in.; biaxial.

and thermal properties than ZnS. The thermal shock resistance parameter given by

$$R' = \frac{s(1-n)k}{aE} \quad (3)$$

where s is the tensile strength, n the Poisson's ratio, k the thermal conductivity, a the coefficient of thermal expansion, and E Young's modulus, was used by Saunders *et al.* [52] to compare the thermal shock behaviour of ZnS and $CaLa_2S_4$. The values in Table XI show that the thermal shock resistance of ZnS is 30 times greater than that of $CaLa_2S_4$.

Covino *et al.* [61], White and co-workers [62, 63] and Chess *et al.* [64] also studied the process of synthesizing calcium lanthanum sulphide using the reaction of alkaline earth carbonates with either oxides or hydroxides of the lanthanum elements at 1100 °C in an atmosphere of flowing H_2S, typical

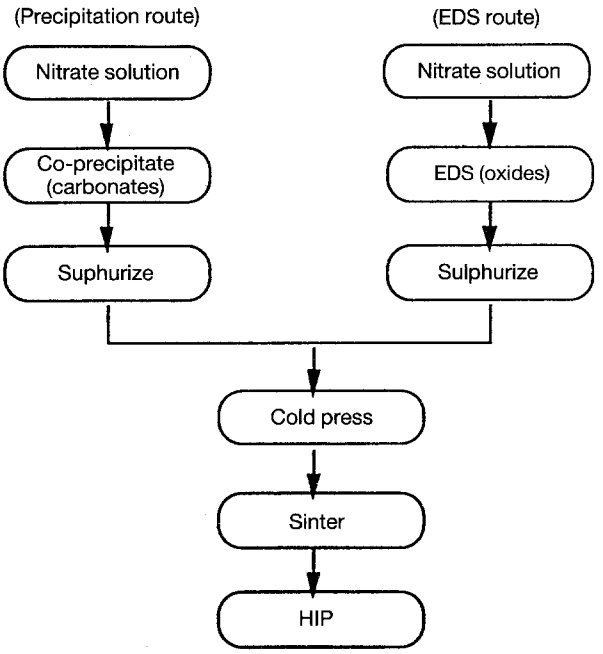

Figure 19 Flow sheet showing the powder synthesis routes for $CaLa_2S_4$ [49, 60].

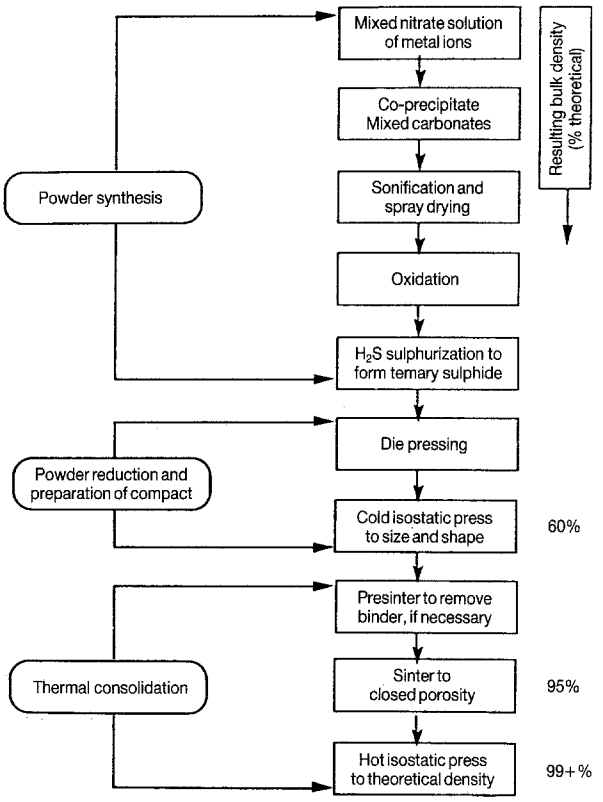

Figure 20 Flow chart showing the various stages in processing of $CaLa_2S_4$ [49, 60].

reaction times being ≈ 3–7 days. However, the ceramic obtained by this method was typically inferior in comparison to the other methods described above. Walker and Ward [65] attempted to grow crystals of ternary sulphides MR_2S_4 (M = Ca, Cd, R = La, Sm, Er). They prepared crystals of $CaLa_2S_4$ using the Stober technique. The technique consisted of directional solidification of the melt at temperatures greater than 2200 °C. The whole molten mass was

contained in a tungsten crucible which was sealed by arc welding. The melts were cooled at a rate of $10\,^{\circ}C\,h^{-1}$ to 1500 °C, and then at $50\,^{\circ}C\,h^{-1}$ to room temperature. The raw materials consisted of starting binary sulphides. However, there were several problems due to volatilization losses of the sulphur, and reaction of the melt with the crucible, resulting in some tungsten precipitates. The powder synthesis methods, however, overcome these problems associated with high-temperature processing.

3.2. Polymorphs of lanthanum sulphide

Lanthanum sulphide exists in several different allotropic forms, namely, α, β and γ. The low-temperature phase, α-La_2S_3 occurs in the orthorhombic form and belongs to the space group *Pnma* with the rare-earth atom site being 8-prismatic and 7-octahedral [45]. It is exactly stoichiometric and stable at low temperatures up to 900 °C. At temperatures above 900 °C, the α form transforms to the β form. Besançon *et al.* [66, 67] showed that the β form of lanthanum sulphide exhibits a tetragonal structure $I4_1/acd$ and is essentially an oxysulphide with the oxygen atoms being substituted by sulphur atoms, to form a solid solution of the formula $La_{10}S_{14}O_{1-x}S_x$. Fig. 21 shows the arrangement of atoms in the β-La_2S_3 cell, the oxygen atoms being at the centre of a tetrahedron of rare-earth atoms. The unit cell with a formula of $(La_{10}S_{14}O)_8$ consists of lanthanum atoms exhibiting two different coordinations of 7 and 8. The 8-fold coordination is similar to that seen in the cubic structure with the arrangement of two sulphur tetrahedra.

Oxygen is in the centre of a symmetric tetrahedron formed of OLa_4 and a particular feature of this structure is an empty cavity between two oxygen atoms which is large enough to receive a sulphur atom. The oxygen atom can be substituted by a sulphur atom, to form a series of solid solution $R_{10}S_{14}O_xS_{1-x}(0 \leq x \leq 1)$ or the sulphur can come into the free cavity while a new lacuna is created in place of oxygen. In this latter case, the lanthanum atoms of the tetrahedron around the oxygen may slightly migrate to make a new tetrahedron around the cavity which would receive the sulphur atom. The range of extent of homogeneity, however, decreases across the lanthanides from lanthanum to samarium with a similar trend seen in the lattice parameters. Oxygen is known to increase the thermal stability of these compounds by increasing their decomposition temperatures. In the case of lanthanum, x can vary from 0–1 and it is the only rare-earth sulphide in which complete substitution of oxygen by sulphur is possible to form β-La_2S_3. Oxygen is known to stabilize the tetragonal phase at low temperatures and hence, its presence plays an important role in the processing of β-La_2S_3 [65].

The cubic (γ) form of lanthanum sulphide occurs in the body centred cubic arrangement and has the defect thorium phosphide structure with metal vacancies. Zachariasen studied the structure of Ce_2S_3 which is isostructural with La_2S_3 and identified the space group for this phase to be $I\bar{4}3d$, the unit cell containing 16 sulphur and $10\frac{2}{3}$ lanthanum atoms, the metal vacancies being randomly arranged such that every ninth position is vacant [44]. The lanthanum atoms are octocoordinated with an unusual environment as shown in Fig. 22. It is a triangular dodecahedron, which can be regarded as formed by the superposition of two tetrahedra, a flat one and an elongated one. By filling up the vacancies, a complete solid solution is obtained form R_2X_3 to the R_3X_4 composition. In the case of R_2X_3, the ionic charges are equilibrated and the compounds have a very high resistivity. In La_3S_4, non-equilibrium of the ionic charges results in metallic behaviour. From the above discussion, it can be seen that La_3S_4 and La_2S_3 are isostructural. They have very similar lattice parameters differing by only 0.06%.

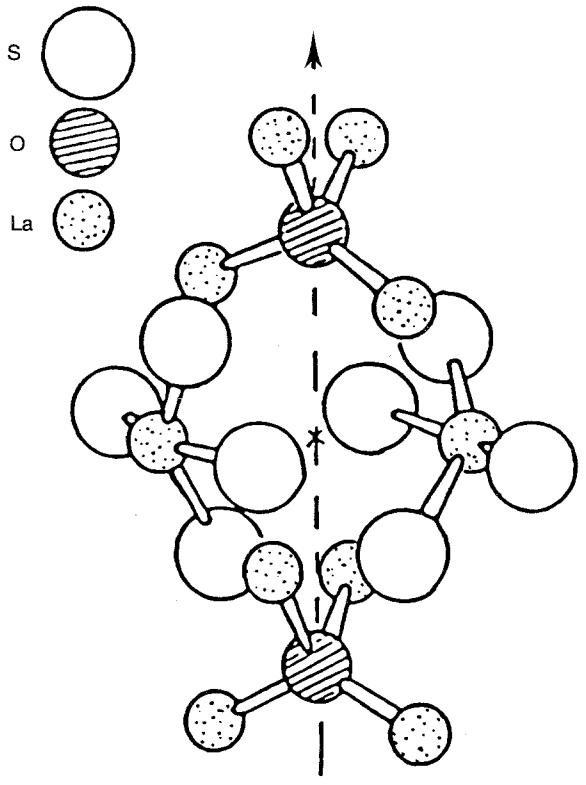

Figure 21 Schematic arrangement of lanthanum, oxygen and sulphur atoms in the tetragonal phase, β-La_2S_3.

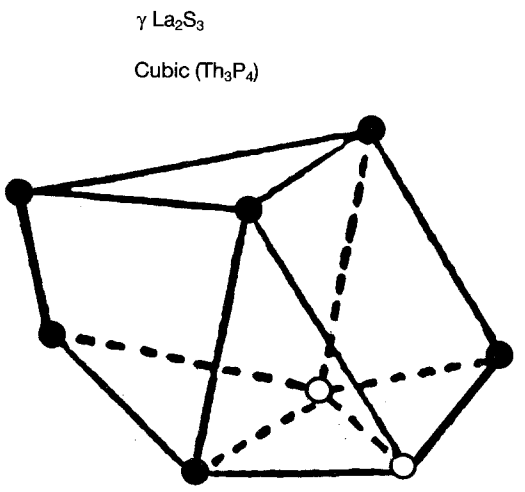

Figure 22 Schematic representation of the unit cell of γ-La_2S_3, which is a triangular dodecahedron formed by the superposition of two tetrahedra. See the text for details [44].

The use of X-ray diffraction to identify the phases could lead to erroneous results [61]. Cubic γ-La_2S_3 is a broad band semiconductor with an optical band gap of about 2 eV. The La_3S_4 form of sulphide has metallic conductivity with one conduction electron per formula unit. Therefore, very small deviations in the stoichiometry of La_2S_3 towards the sulphur deficient La_3S_4 produce "dirty" semiconductor-type behaviour.

3.3 Conventional processing of cubic (γ) lanthanum sulphide

The cubic form of lanthanum sulphide (γ), being iso structural with $CaLa_2S_4$ shows potential for use as an optical window in the 8–14 μm range. Cubic lanthanum sulphide was synthesized by Gschneidner and co-workers [68–73] in a number of ways. One of the easiest methods used was to react the oxide of lanthanum in flowing H_2S at temperatures of 1350 °C to form the cubic phase of lanthanum sulphide. This method was also reported by Henderson *et al.* [74]. There was always a problem of incomplete reaction. In the other most commonly used method, elemental lanthanum and sulphur are reacted in a quartz ampoule to form α-La_2S_3. These reactions were typically conducted for a period of 24 h at 600 °C and 3 days at 950 °C. After completion of the reaction, the quartz ampoules were opened in a helium-filled glove box and the reaction products (LaS and La_2S_3) were ground and placed in tungsten crucibles.

The crucibles and the contents were heated under vacuum to 1500 °C and then to 2150 °C under an argon atmosphere to melt and homogenize. The high-temperature heat treatments resulted in the formation of the cubic lanthanum sulphide powders. The powders obtained were then sintered by a technique known as the pressure-assisted reaction sintering (PARS) technique. This technique consists of mixing the La_2S_3 powders with the hydride (LaH_3) in the desired composition and heating the sample in a die with the application of pressure, the chamber being initially maintained at a vaccum of 10^{-3} torr. At a temperature of 800 °C, the hydride decomposes, resulting in the formation of highly reactive lanthanum metal. The hydrogen gas evolved is pumped off from the system. The lanthanum metal then forms a liquid phase that helps to densify the powders along with subsequent reaction to form the cubic phase at 1450 °C. Samples were sintered to 97% theoretical densities using this technique [73].

Wood *et al.* [75], and Whittenberger and Smoak [76] also prepared this phase by a similar process. They prepared the α-phase in a manner similar to the method used by Gschneidner and then hot pressed the lanthanum sulphide powders at 1527 °C in vaccum. Whittenberger and Smoak [76] reported presence of mixed phases of β and γ forms of lanthanum sulphide in their hot-pressed samples. Table XII summarizes the various methods employed to synthesize the cubic phase. All the above methods of synthesis employed to prepare the cubic phase pertain to the investigation of the thermoelectric properties of lanthanum sulphide. Apart from structural studies and measurement of thermoelectric properties at high temperatures, very little has been reported on its optical properties [46,77–90]. Its optical properties were only investigated by Volynets *et al.* [78]. They synthesized the γ-phase by sulphidizing the oxide at high temperature using carbon disulphide as the sulphidizing agent and then densifying the powders by hot pressing at temperatures of 1000–1300 °C. They observed 65% transmission in the range of 14 μm. Single crystals of cubic lanthanum sulphide were prepared by Kamarzin *et al.* [91] in a specially designed reaction vessel by maintaining the melt in a continuous dynamic atmosphere of sulphur. The single crystals exhibited a transmission cut-off at 20 μm as shown in Fig. 23.

3.4 Conventional processing of tetragonal (β) lanthanum sulphide

Besançon [66] first studied the structure of this tetragonal intermediate phase using X-ray diffraction and determined that it is an oxysulphide with the formula $La_{10}S_{14}O$. He synthesized this phase by reacting lanthanum oxide with γ or α-La_2S_3 in stoichiometric

TABLE XII Conventional synthesis of γ-La_2S_3

Synthesis method	Reaction conditions	Refs.
Melting and solidification		
1. Melt La and S in an evacuated quartz ampoule to form α-La_2S_3	600 °C for 24h	[68–73]
2. α-$La_2S_3 \rightarrow \beta$-$La_2S_3$	950 °C for 3 days	[75, 76]
3. β-$La_2S_3 \rightarrow \gamma$-$La_2S_3$	1500 and 2150 °C in an evacuated sealed tungsten crucible	
Gas–solid reaction		
1. Synthesis of lanthanum oxide by decomposition of lanthanum carbonate	Aqueous precipitation at room temperature	[74]
2. $La_2O_3 + 3H_2S \rightarrow La_2S_3(\beta,\gamma)$	Sulphidization at 1350 °C for 7 days	[54]

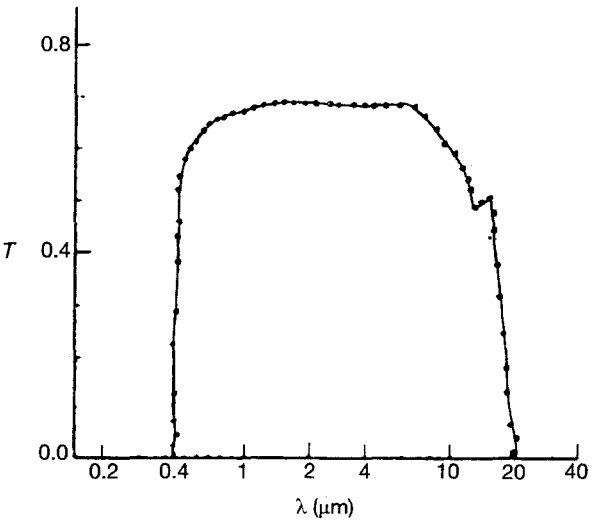

Figure 23 Transmission spectrum of single-crystal γ-La_2S_3 showing the IR cut-off at 20 μm [91].

proportions at about 1000 °C. Lewis *et al.* [57] and Savage *et al.* [56] also synthesized this material by preparing the oxide using the EDS method and, after drying, sulphidizing the oxide in a H_2S/N_2 atmosphere for 15 h at 1000 °C. The powders obtained were then sintered to near theoretical density by hot pressing in argon atmosphere using a titanium–zirconium–molybdenum alloy die and high-density graphite punches. Pressures up to 10 p.s.i. (10^3p.s.i. = 6.89N mm^{-2}) were used with pressure being applied for 20 min. The transmission spectrum obtained showed a broad absorption at 9.1 μm due to the presence of molecular SO_4^{2-} complex (see Fig. 24).

3.5. Chemical processing of sulphide ceramics

The sections above described the traditional methods that were used for the synthesis of these rare-earth sulphides. Most of the methods involved processing the sulphide from the melt or by using gas–solid reactions to form the sulphide. Melt processing of these materials is certainly not impossible as described above, but the vapour pressures and the high melting point of the rare-earth sulphides makes it extremely difficult to achieve good compositional homogeneity and controlled grain size without contamination from the crucible [92–94]. Chemical processing of these refractory materials offers several advantages that could be exploited for the synthesis of optical materials. Several wet chemical techniques are reported in the literature such as precipitation, microemulsion synthesis, colloidal processing and sol–gel synthesis, along with hydrothermal processing. There has been a considerable amount of work reported in the literature on these techniques and references [95–128] contain valuable information on the principles and various modifications of the solution techniques to synthesize ultrafine powders that result in fine-grained ceramics. However, most of the information available is on the application of the techniques for the synthesis of oxide materials and the use of similar synthesis routed for the preparation of non-oxide sulphide materials is very scarce.

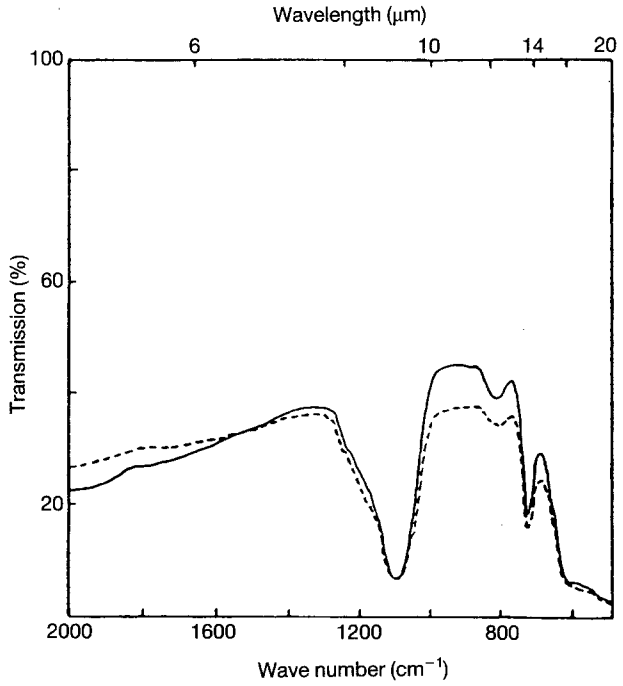

Figure 24 Infrared transmission of sintered β-La_2S_3 samples, (- - -) hot pressed at 1100 °C, 20 min and (———) annealed at 1100 °C in H_2S for 4 h. Note the absorption at 9.1 μm due to the presence of molecular SO_4^{2-} complex [27].

Melling [115] reported preparation of amorphous germanium sulphide by application of the sol-precipitation technique which is essentially precipitation from the alkoxide solution of germanium. The sol was reacted with H_2S to obtain germanium sulphide powders. By controlling the solvent to reactant ratio and the temperature, a wide range of amorphous, crystalline and partially crystalline powders could be obtained. Matijevic and Wilhelmy [116] also reported preparation of monodispersed spherical colloidal particles of cadmium sulphide. These particles were synthesized by first preparing cadmium sulphide "seeds" which were precipitated by ageing a solution consisting of cadmium nitrate, nitric acid and thioacetamide. By adding varying amounts of thioacetamide to this solution, the "seed" crystals were allowed to grow to give uniform monodispersed spherical particles of smooth surface with an average size of 0.7 μm. At the same time there is work in the literature [129] on use of microemulsion technique for the preparation of fine particles of CdS, CdSe, and In_2S_3 for quantum well application.

All these novel techniqes result in ultrafine powders which are generally amorphous in the as-prepared state. The ultrafine size (nanometre range) of these powders made them very reactive in subsequent processing reactions such as ammonialysis and sulphidization. Furthermore, the amorphous character of the precursors often results in the formation of phases that are otherwise difficult to obtain by conventional equilibrium synthesis techniques. The inherent problems of contamination which come into play from the raw materials in aqueous chemical techniques for synthesis of non-oxides, typically the hydroxides, can be overcome by the use of metallorganics. The metallorganic compounds are typically liquids with low boiling points or solids with low melting points. They can be distilled and redistilled to be obtained in very high purity. As a result, chemically homogeneous, fine particles of very high purity can be synthesized. The use of these precursors for synthesis of non-oxide ceramics is, therefore, very attractive. In addition, the high reactivity of the metallorganics, particularly in the case of the rare-earths make them especially useful for synthesizing fine sulphide powders that can be densified into a ceramic. There has been very limited work on the use of the alkoxides for the synthesis of sulphides, while some work has been reported on the use of organometallic precursors to form ZnS powders and the sintered ceramic [130–135]. There have also been reports on the use of tert-butyl sulphide for the preparation of crystalline sulphides in the Ti–S system [136]. However, there is no work in the literature on the use of metallorganic precursors for the synthesis of lanthanum sulphide.

3.6. Chemical processing of cubic (γ) and tetragonal (β) lanthanum sulphide

We have successfully demonstrated the use of lanthanum alkoxide for the synthesis of fine amorphous oxysulphide precursor particles that transform at low temperatures to form cubic and tetragonal lanthanum sulphide. Lanthanum alkoxide was used as the starting chemical based on the fact that the alkoxide molecules are extremely reactive and the high polarity of the alkoxy (OR^- where R = alkyl radical) groups leave the metal atom susceptible to nucleophilic attack. Depending on the nature of the nucleophile, the substitution reaction can be controlled by the use of catalyst to result in the formation of gels or extremely fine nanometre size particles.

The chemistry of the rare-earth metals is very similar to group III elements and hence sulphidization of salts of lanthanum in an aqueous medium results in the formation of hydroxides rather than sulphides, while sulphidization of salts of lanthanum in non-aqueous solvents results in substantial oxygen retention [137] thereby preventing its use for synthesis of sulphides for window technology. The alkoxide route was chosen despite the high oxyen content of the starting alkoxide compounds because of its high reactivity and the fine particle-sized nature of the oxysulphide precursor that is generated. This makes it amenable for subsequent sulphidization reactions, substantially reducing the oxygen content. We have successfully demonstrated the use of lanthanum alkoxide for the synthesis of ultrafine oxysulphide precursors that transform to cubic lanthanum sulphide.

Cubic lanthanum sulphide powders were synthesized from lanthanum alkoxide sols [11, 12]. The sols were sulphidized using H_2S at room temperature to generate oxysulphide precursors that are extremely fine ≈ 20 nm in size as shown in Fig. 25. These precursors are amorphous with a specific surface area of 74.34 $m^2\ g^{-1}$m and on sulphidization at 1000 °C for 8 h result in the formation of cubic La_2S_3. The flow sheet for the synthesis is shown in Fig. 26. The resulting cubic La_2S_3 particles are 1–3 μm in size with rounded and smooth surfaces indicating the occurrence of viscous flow due to the amorphous to crystalline transition during heat treatment (see Fig. 27). Chemical analysis indicates the precursors to contain 8.50 wt % sulphur and is shown in Table XIII. The oxysulphide precursors on heat treatment in inert conditions transform to La_2O_2S, indicating the bonded nature of the sulphur. The retention of only ≈ 8.50 wt % in the precursor suggests the inability of the sulphur to replace completely the alkoxy groups and this can be envisioned from the fact that H_2S is a weak acid with a pK_a of 7.04. This, therefore, makes the availability of stoichiometric amounts of the SH^- nucleophiles very difficult in the presence of an inert solvent medium, and hence the complete replacement of all the alkoxy groups with SH^- becomes very remote. Based on this, the sulphidization reaction has been proposed as follows

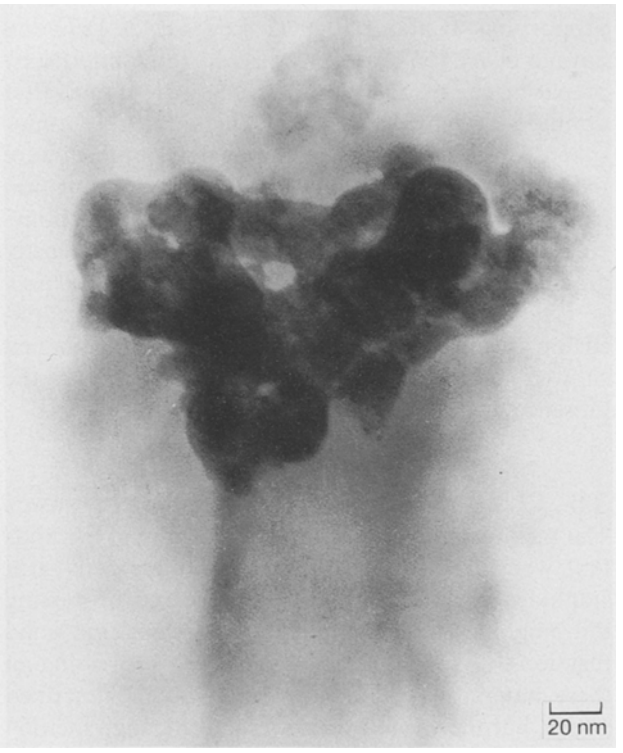

Figure 25 Transmission electron image showing the interconnected fine particles (≈ 20 nm) of the alkoxy-sulphide precursors used to synthesize γ-La_2S_3.

$$La(OC_3H_7)_3 + xH_2S \rightarrow La(OC_3H_7)_{3-x}(SH)_x + xC_3H_7OH \qquad x = 1\text{–}3 \qquad (4)$$

According to the above reaction, 3 mol H_2S should be sufficient to replace all the alkoxy groups; however, only partial replacement is seen.

The incomplete sulphidization reaction results in the formation of an oxysulphide. However, the amount of sulphur in the precursor and the oxygen to

TABLE XIII Chemical analysis of sulphide precursor and transformed cubic lanthanum sulphide and oxysulphide powders

Element	As-prepared precursor	Oxysulphide (observed)	γ-LaS_3 (observed)	La_2S_3 (theoretical)
La	50.05 ± 2	66.06 ± 5	74.31 ± 2	74.32
S	8.50 ± 0.5	10.62 ± 0.3	25.71 ± 0.5	25.68
C	5.96 ± 0.01	0.32 ± 0.01	0.05 ± 0.01	–
H	1.79 ± 0.01	0.15 ± 0.01	< 0.02 ± 0.01	–
O	33.7[a]	NA[b]	NA[b]	–

[a] Estimated to be the balance.
[b] Not analysed.
Note:Theoretical wt % for La_3S_4 are 76.5 wt % for La and 23.5 wt % for S.

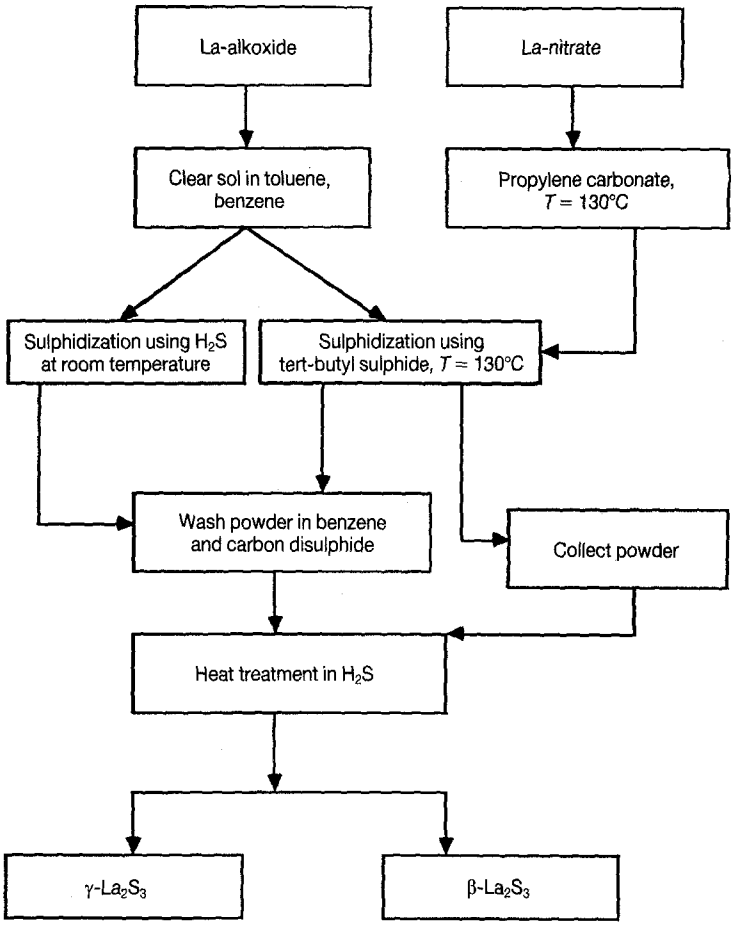

Figure 26 Flow sheet showing the processes followed for the synthesis of γ-La_2S_3 and β-La_2S_3.

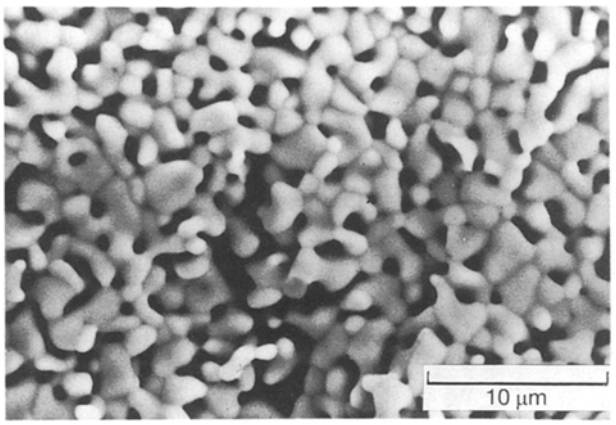

Figure 27 Scanning electron micrograph showing the transformed γ-La_2S_3 particles, 1–3 μm in size. The micrograph shows the particles to have undergone some viscous flow due to the amorphous to crystalline transition resulting in rounded smooth surfaces and partial sintering.

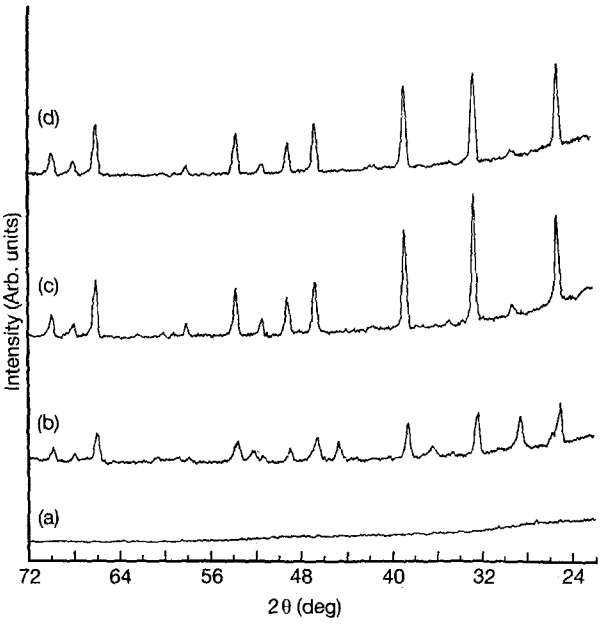

Figure 28 XRD traces showing the evolution of the cubic phase (γ-La_2S_3) on heat treating the precursor at 1000 °C in H_2S for different time intervals. (a) As-prepared; (b) 3 h, 1000 °C, La_2O_2S, and γ-La_2S_3, in H_2S atmosphere, (c) additional 4 h, 1000 °C, γ-La_2S_3, in H_2S atmosphere; (d) 8 h, 1000 °C, γ-La_2S_3, in H_2S atmosphere.

sulphur ratio is very important for the conversion of the oxysulphide to the cubic rare-earth sulphide. A S/O ratio of 0.25 has been found to be essential for the formation of the cubic sulphide. The transformation of the oxysulphide precursor to the cubic sulphide has been shown to occur on heat treating the precursors at 1000 °C for 8 h. The evolution of the phases is shown in Fig 28.

An interesting observation is the formation of the oxysulphide, La_2O_2S and γ-La_2S_3 on heating the precursor at 1000 °C for 4.5 h. This is an indication that the oxysulphide precursor could be potentially forming the cubic phase at much lower temperatures. Vaughan and White [138] have shown in their study

based on the existing data in the literature that La_2O_2S and the cubic (γ) form of the sulphide are stable only at 1450–1500 °C and at temperatures below it is the tetragonal (β) phase and the oxysulphide which remain stable. Thus, the precursor plays an important role in the kinetics of formation of the cubic phase. Current on-going research in our group should provide more insight into these reactions. These results demonstrate the applicability of the alkoxides as powerful precursors for synthesizing novel rare-earth sulphides. Following our work, there have been quite a few reports on the use of alkoxides for the synthesis of $CaLa_2S_4$ [139–143].

It is clear that the fine particle size and the amount of sulphur incorporated into the chemically generated oxysulphide precursor are both responsible for the formation of the cubic phase at low temperatures. The chemical reactions conducted in solution allow for faster diffusion of molecular species due to the reduced diffusional distances, thereby favouring excellent molecular mixing. Good compositional homogeneity is, therefore, achieved in the final product. Moreover, the molecular arrangement of ions in solution can be changed depending on the reaction conditions such as pH, temperature, and type of solvent resulting in the formation of non-equilibrium phases. Thus, the solution techniques, similar to the rapid solidification techniques also lead to formation of novel non-equilibrium phases in ceramic systems. Recently, there have also been some reports on the use of mechanical alloying technique to generate metastable phases. This process, also called attrition milling, has been applied by Gschneidner *et al.* [144, 145] in synthesizing high-pressure phases in rare-earth sulphides (γ-R_2S_3, R = Er, Tm, Yb, Lu, Y and Dy). They have shown that by mechanically milling powders of the sulphide, either a metastable crystalline high-temperature polymorph, γ-Dy_2S_3 or a metastable high-pressure phase (γ-Y_2S_3) could be synthesized at room temperature [144].

The tetragonal (β) lanthanum sulphide powders have been synthesized by us using chemical techniques analogous to those used for the preparation of the cubic phase [13–15]. Two different precursors were synthesized which transformed to the β-phase upon heat treatment in H_2S. The flow sheet for the two synthesis procedures are outlined in Fig. 26. The first procedure incorporated the use of the alkoxide which was sulphidized using H_2S for $\approx$ 1.5 h as opposed to 4 h in the case of the cubic sulphide. In the other route, lanthanum nitrate hexahydrate was used which was dissolved in propylene carbonate, the sulphidizing agent used was tert-butyl sulphide. Both the precursors were amorphous and showed similar characteristics as the cubic sulphide precursor. But on heat treatment in H_2S at 1000 °C, the precursors transform to generate the tetragonal phase of lanthanum sulphide. Chemical analysis indicated that the precursors contained only $\approx$ 5 wt % sulphur. The amount of sulphur in the precursor and the ratio of S/O, therefore, determines the formation of the two different phases. The amount of sulphur that could be incorporated into the alkoxide network would depend on the prehydrolysed state of the alkoxide. Prehydrolysis would imply that some of the alkoxy groups are replaced by OH – preventing the nucleophilic attack of lanthanum by SH – thereby reducing the sulphur content in the precursors. A lower amount of sulphur incorporated in the gel structure would imply the precursors to be richer in oxygen which results in the formation of the tetragonal phase, in accordance with the studies of Besançon [66, 67]. Sulphidization of the gels can, therefore, be monitored accordingly, to result in the formation of the cubic or tetragonal phases. Fig. 29 and 30 show the micrographs of the tetragonal lanthanum sulphide precursor and the transformed β-La_2S_3 powders. Thus, the alkoxides are powerful precursors to synthesize sulphides of reactive metals as described above, and the approach is currently being extended to even synthesize transition metal sulphides. More information pertaining to the synthesis and the affect of the chemistry of the precursors on the formation of the two phases can be obtained in the literature [12–14].

The cubic lanthanum sulphide powders were hot pressed and preliminary transmission results obtained by us on polished 0.9 mm thick discs is shown in Fig. 31. The spectra shows that the cubic phase transmits up to $\approx$ 13 μm. Although the per cent transmittance is not yet acceptable for optical application, the results are encouraging and more work is warranted to improve this material for window applications. The hot-pressed samples show an average grain size of $\approx$ 6.0 μm indicating a two-fold increment in the grain sizes from the powder stage of $\approx$ 3 μm but the presence of porosity could be the reason for the diminished percentage of transmission. The research is in

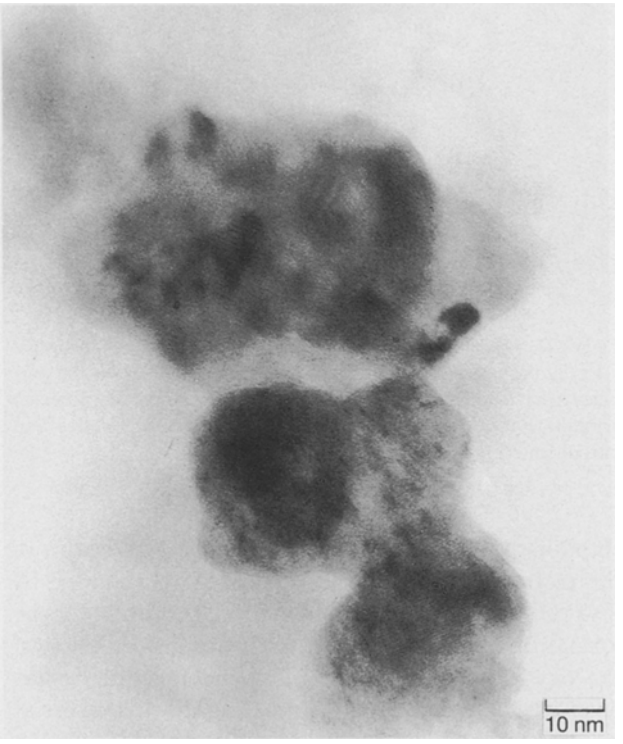

Figure 29 Transmission electron micrograph showing the ultrafine ($\approx$ 20 nm) particles of the oxysulphide precursors used to synthesize β-La_2S_3.

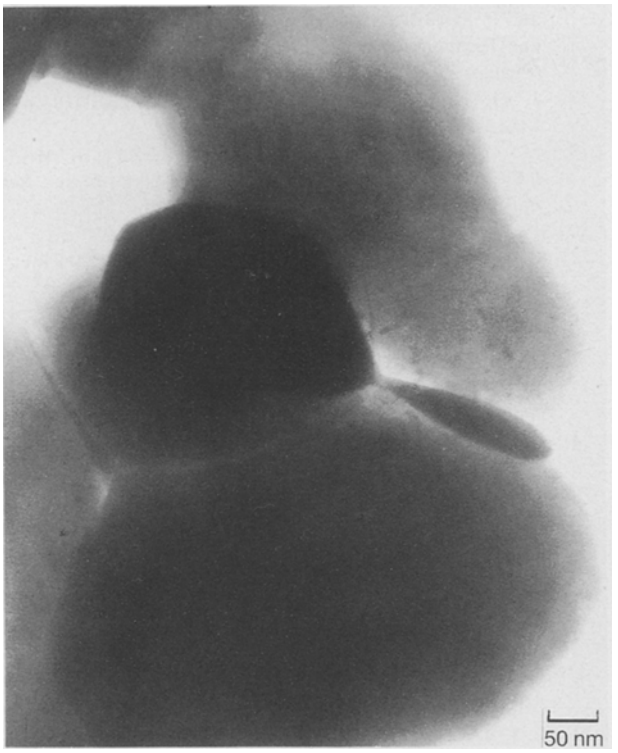

Figure 30 Transmission electron brigh-field image of transformed β-La_2S_3 particles showing 0.5–1.0 μm size particles.

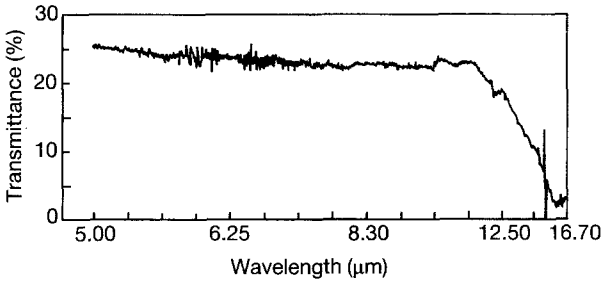

Figure 31 Transmission spectra obtained on hot-pressed γ-La_2S_3 sample (0.9 mm thick). The spectrum shows the IR cut-off to be at ≈ 13 μm.

the preliminary stage of developments and the results are quite promising. More work in this direction is still being carried out, particularly on the structural characterization of the alkoxy-sulphide gels and the transformation kinetics of the precursors to the sulphide ceramic.

3.7 Current status of rare-earth sulphides in optical windows

There is much research that is needed to be performed in the area of chemical processing of the rare-earth sulphides. The complex chemistry and the extreme affinity for oxygen makes chemical processing of these materials very difficult. White and co-workers [146–149] in their recent work using Raman spectroscopy has shown the complex chemistry of these materials. The successful synthesis routes established by the authors provides impetus for further research to be conducted on the reaction pathways and the nature of the precursor which plays such a crucial role in the transformation of the oxysulphide to the desired sulphide phase. Moreover, there is a need to identify other types of chemical reactions that can result in the formation of La_2S_3 directly at low temperatures. However, the exacting requirements that the materials need to fulfil in order to be applicable as IR windows always leaves the door open for a better and more perfect material. Progress in ceramic processing and the understanding of materials chemistry led to the discovery and development of the chalcogenides and the rare-earth sulphides. The large thermal expansion coefficients and the high softening temperatures of the chalcogenides paved the way for the alkaline earth–rare-earth sulphides which were better but still not the best. The rare-earth sulphides again possess better physical, chemical and optical attributes than those possessed by the ternary rare-earth–alkaline-earth sulphides. However, with the advent of diamond films there is a major change that one may foresee in the near future which may render the rare-earth sulphides obsolete for infrared window application.

Diamond is a material which exhibits several unique properties. Table VI lists its properties along with the existing transmitting materials [150, 151]. Among others, the property most useful for optical application is its wide transmission that spans the ultraviolet–visible–far-infrared region. It exceeds boron nitride (BN) in hardness and conducts heat five times better than silver and has only 40% density of copper. These properties make it very unique, and certainly the most sought-after material for window application. Bulk synthesis of this material is very difficult and requires high temperatures and pressures, but the advancement in thin-film technology has led to a breakthrough in diamond thin-film synthesis. Several articles can be obtained in the literature in regard to processing of thin films of diamond using metastable reaction conditions to produce these films at temperatures as low as 300 °C and even lower. This technology is being used to coat the existing infrared materials with diamond. The usefulness of this material has resulted in significant research in the development of free-standing diamond so that the actual windows could be made of diamond in the future. The advent of diamond, therefore, may render the use of the rare-earth sulphides obsolete for the 8–14 μm window technology, but nevertheless, these materials would still be useful for optical and electronic applications. Recent work by Vanderah and co-workers [152, 153] indicates that sulphide materials could still be promising materials for window applications in the two-colour 3–5 μm and 8–14 μm spectral regions, because diamond tends to absorb in the 3–5 μm spectral range.

4. Conclusion

In this review we have discussed the emergence of the rare-earth sulphides as promising infrared materials both in the amorphous and crystalline state. Inasmuch as the useful properties exhibited by rare-earth sulphide-based glasses, there are several intriguing questions pertaining to the structure, phase diagram and properties that still remain to be solved in these novel glass

systems. There is à need to focus and understand in greater detail the immiscibility in these systems and to investigate the effect of phase-separation on the optical properties. The structure of the glass and the role of the rare-earth atom in the sulphide environment should also be probed, similar to the Ga_2S_3–La_2S_3 glasses. Research in these directions would definitely contribute and enhance the growth and knowledge of this developing area of rare-earth glass science and technology. Chemical processing of crystalline rare-earth sulphides still warrants considerable research in the direction of understanding the mechanism for the formation of the precursor and the transformtion of the precursor to the final sulphide ceramic. The structure of the precursor would need considerable scrutiny and there is definitely an increasing need to optimize the processing routes to increase the sulphur yield in the precursor and find suitable reagents or chemical reaction parameters that would eventually result in the formation of the sulphide at temperatures as low as room temperature. In view of the interesting optical properties, several novel ternary systems containing the rare-earth sulphides could be envisioned.

Acknowledgements

This review article is based on a part of the Ph D work of Prashant N. Kumta. The authors thank Professor K. A. Gschneidner and Professor W. B. White for providing information useful for this review. The authors acknowledge the National Science Foundation, Grant DMR87-03721 under the electronics materials program of the Division of Materials Research, for supporting this work.

References

1. H. RAWSON, in "Inorganic Glass-Forming Systems" (Academic Press, New York, 1967) p. 249.
2. N. J. KREIDL, in "Glass Science and Technology", Vol. 1, "Glass-Forming Systems", edited by D. R. Uhlmann and N. J. Kreidl (Academic Press, New York, 1983) p. 231.
3. J. A. SAVAGE, *J. Non-Cryst. Solids* **47** (1982) 101.
4. A. PEARSON, in "Modern Aspects of the Vitreous State", edited by J. Mackenzie (Butterworths, London, 1964) p. 29.
5. S. DEMBOVSKII, *Inorg. Mater.* **5** (1969) 385.
6. P. N. KUMTA and S. H. RISBUD, *Bull. Am. Ceram. Soc.* **69** (1990) 1977.
7. A. R. HILTON, C. E. JONES and M. BRAU, *Phys. Chem. Glasses* **7** (4) (1966) 05.
8. W. H. DUMBAUGH, *Opt. Eng.* **24** (1985) 257.
9. Y. KAWAMOTO and S. TSUCHIHASHI, *J. Am. Ceram. Soc.* 52 (1969) 626.
10. *Idem, ibid.* **54** (1971) 131.
11. P. N. KUMTA and S. H. RISBUD, *Mater. Sci. Eng.* **B2** (1989) 281.
12. *Idem, J. Mater. Res.* **8** (1993) 1394.
13. *Idem, Prog. Cryst. Growth. and Char. of Mater.* **22** (1991) 321.
14. *Idem, Mat. Sci. Eng. B* **18** (1993) 260.
15. *Idem*, in "Proceedings of the 4th International Conference on Ultrastructure Processing of Glasses, Ceramics and Composites," Tucson, AZ, February 1989, edited by D. R. Uhlmann and D. R. Ulrich (Wiley, New York, 1992) p. 555.
16. S. BARNIER, M. GUITTARD, M. P. PARDO, A. M. LOIREAU-LOZAC'H and JEAN FLAHAUT, *Mater. Res. Bull.* **18** (1983) 1217.
17. A. BORNSTEIN, J. FLAHAUT, M. GUITTARD, S. JAULMES, A. M. LOIREAU-LOZAC'H, G. LUCAZEAU and R. REISFIELD, in "The Rare Earths in Modern Science and Technology," edited by G. J. McCarthy and J. J. Rhine (Plenum Press, New York, 1978) p. 599.
18. J. FLAHAUT, M. GUITTARD and A. M. LOIREAU-LOZAC'H, *Glass Technol.* **24** (3) (1983) 49.
19. M. GUITTARD, A. M. LOIREAU-LOZAC'H, M. P. PARDO, J. FLAHAUT and G. LUCAZEAU, *Mater. Res. Bull.* **13** (1978) 317.
20. P. LARUELLE, *Ann. Chim. (Paris)* **7** (1982) 119.
21. C. CARCALLY, M. GUITTARD and A. M. LOIREAU-LOZAC'H, *Mater. Res. Bull.* **15** (1980) 545.
22. A. M. LOIREAU-LOZAC'H, S. BARNIER, M. GUITTARD, P. BESANÇON and J. FLAHAUT, *Ann. Chim.* **9** (1974) 127.
23. L. CERVINKA and A. HRUBY, *J. Non-Cryst. Solids* **48** (1982) 231.
24. A. M. LOIREAU-LOZAC'H, M. GUITTARD and J. FLAHAUT, *Mater. Res. Bull.* **12** (1977) 881.
25. *Idem, ibid.* **11** (1976) 1489.
26. M. J. WEBER, in "Proceedings of the International Conference on Lasers", edited by R. C. Powell (STS Press, New Orleans, LA, 1982).
27. S. BENAZETH, M. H. TUILIER, A. M. LOIREAU-LOZAC'H, H. DEXPERT, P. LAGARDE, and J. FLAHAUT, *J. Non-Cryst. Solids* **110** (1989) 89.
28. M. GUITTARD, P. H. FOURCROY, J. FLAHAUT and A. CHILOUET, *Ann. Chim.* **1** (1976) 47.
29. P. S. BARNIER, M. GUITTARD and J. FLAHAUT, *Mater. Res. Bull.* **14** (1979) 973.
30. P. N. KUMTA and S. H. RISBUD, in "Proceedings of the SPIE Convention", San Diego, CA 8-13 July. Edited by A. J. Marker (SPIE, 1990) p. 10.
31. *Idem, J. Mater. Res.* **6** (1991) 2694.
32. E. S. SARKISOV, R. A. LIDEN and V. V. SHUM, *Izv. Akad. Nauk SSSR Neorg Mater.* **6** (1970) 20544.
33. P. N. KUMTA, Ph D dissertation, University of Arizona, Tucson, AZ (1990).
34. E. R. PLUMAT, *J. Am. Ceram. Soc.* **51** (1968) 499.
35. K. WEI, J. WENZEL, E. SNITZER and G. H. SIGAL Jr, "in 94th Annual Ceramic Society Meeting", Abstract 71-G, Minneapolis (1992) p. 238.
36. J. A. SAVAGE, in "Infrared Optical Materials and their Antireflection Coatings" (Adam Hilger, London, 1985) p. 3.
37. J. A. SAVAGE and K. J. MARSH, *Proc. SPIE* **297** (1981) 35.
38. P. KLOCEK, *MRS Bull.* **5** (1986) 41.
39. S. MUSIKANT, "Optical Materials, an Introduction to Selection and Application" (Marcel Dekker, New York, 1985).
40. P. E. D. MORGAN and M. S. KOUTSOUTIS, *Mater. Res. Bull.* **22** (1987) 617.
41. R. W. G. WYCKOFF, *Crystal Struct.* **II** (1964) 160.
42. *Idem, Ibid.* **II** (1964) 75.
43. D. ROY, *SPIE Proc.* **297** (1981) 24.
44. W. H. ZACHARIASEN, *Acta Crystallogr.* **2** (1949) 57.
45. J. FLAHAUT, in "Handbook on the Physics and Chemistry of Rare Earths", Edited by K. A. Gschneidner Jr. and Le RoyEyning, Vol. 4 (North-Holland, Amsterdam, 1979) p. 1.
46. J. FLAHAUT, M. GUITTARD, M. PATRIE, M. P. PARDO, S. M. GULABI and L. DOMANGE, *Acta Crystallogr.* **19** (1965) 14.
47. C. LOWE-MA, in "Advances in Materials Characterization", edited by D. R. Rossington, R. A. Condrate and R. L. Snyder (Plenum, New York, 1983) p. 267.
48. A. W. SLEIGHT and C. T. PREWITT, *Inorg. Chem.* **7** (1968) 2282.
49. K. J. SAUNDERS, T. Y. WONG. T. M. HARTNETT, R. W. TUSTISON and R. L. GENTILMAN, *SPIE Proc.* **683** (1986) 72.
50. D. C. HARRIS, M. E. HILLS, R. L. GENTILMAN, K. J. SAUNDERS and T. Y. WONG *Adv. Ceram. Mater.* **2** (1987) 74.
51. W. M. YIM, A. K. FAN and E. J. STOFKO, *J. Electrochem. Soc. Solid State Sci. Technol.* **120** (1973) 441.
52. K. J. SAUNDERS, T. Y. WONG, R. L. GENTILMAN, *Proc. SPIE* **505** (1984) 31.

53. D. L. CHESS, C. A. CHESS and W. B. WHITE, *J. Am. Ceram. Soc.* **66** (1983) C 205.
54. O. SCHEVCIW and W. B. WHITE, *Mater. Res. Bull.* **18** (1983) 1059.
55. D. L. CHESS, C. A. CHESS and W. B. WHITE, *ibid.* **19** (1984) 1551.
56. J. A. SAVAGE, K. L. LEWIS, B. E. KINSMAN, A. R. WILSON and R. RIDDLE, *Proc. SPIE* **683** (1986) 79.
57. K. L. LEWIS, J. A. SAVAGE, K. J. MARSH and A. P. C. JONES, *ibid.* **400** (1983) 21.
58. J. A. BESWICK, D. J. PEDDAR, J. C. LEWIS and F. W. AINGER, *ibid.* **400** (1983) 12.
59. R. L. GENTILMAN, M. B. DEKOSKY, T. Y. WONG and R. W. TUSTISON, *Proc. SPIE* **929** (1988) 57.
60. M. E. HILLS, "Preparation, Properties and Development of Calcium Lanthanum Sulfide as an 8-12 μm Transmitting Ceramic", Naval Weapons Center, China Lake, CA (1989).
61. J. COVINO, D. C. HARRIS, M. E. HILLS, R. T. LODA and R. W. SCHWARTZ, *Proc. SPIE* **505** (1984) 42.
62. W. B. WHITE, D. CHESS, C. A. CHESS, J. V. BIGGERS, *ibid.* **297** (1981) 38.
63. P. C. PROVENZANO, S. I. BOLDISH and W. B. WHITE, *Mater. Res. Bull.* **12** (1977) 939.
64. D. L. CHESS, C. A. CHESS, J. V. BIGGERS and W. B. WHITE, *J. Am. Ceram. Soc.* **66** (1983) 18.
65. P. J. WALKER and R. C. C. WARD, *Mater. Res. Bull.* **19** (1984) 717.
66. P. BESANÇON, D. CARRE, P. LARUELLE and J. FLAHAUT, in "Proceedings of the 9th Rare-Earth Conference", Vol. 1, edited by P. E. Field (Blacksburg, VA, 1971) p. 113.
67. P. BESANÇON, *J. Solid State Chem.* **7** (1973) 232.
68. K. A. GSCHNEIDNER Jr, J. F. NAKAHARA, B. J. BEAUDRY and T. TAKESHITA, *Mater. Res. Soc. Symp.* **97** (1987) 359.
69. T. AMANO, B. J. BEAUDRY and K. A. GSCHNEIDNER *J. Appl. Phys.* **59** (1986) 3437.
70. T. TAKESHITA, B. J. BEAUDRY and K. A. GSCHNEIDNER Jr, in "The Rare Earths in Modern Science and Technology", 3, edited by G. J. McCarthy, H. B. Silber and J. J. Rhyne, (Plenum, 1982) p. 255.
71. T. TAKESHITA, B. J. BEAUDRY and K. A. GSCHNEIDNER Jr, in "Fourth International Conference on Thermoelectric Energy Conversion", edited by K. R. Rao (Institute of Electrical and Electronic Engineers, New York, 1982) p. 48.
72. B. J. BEAUDRY, M. J. TSCHETTER, J. F. NAKAHARA, T. TAKESHITA and K. A. GSCHNEIDNER Jr, in "Sixth International Conference on Thermoelectric Energy Conversion", The University of Texas at Arlington, edited by K. R. Rao 12-14 March (University of Texas, Arlington, 1986) p. 20.
73. T. TAKESHITA, K. A. GSCHNEIDNER Jr and B. J. BEAUDRY, *J. Appl. Phys.* **57** (1985) 4633.
74. J. R. HENDERSON, M. MURAMOTO, E. LOH and J. B. GRUBER, *J. Chem. Phys.* **47** (1967) 3347.
75. C. WOOD, A. LOCKWOOD, J. PARKER, A. ZOLTAN and D. ZOLTAN, *J. Appl. Phys.* **58** (1985) 1542.
76. J. D. WHITTENBERGER and R. H. SMOAK, *J. Am. Ceram. Soc.* **70** (1987) C-90.
77. S. M. LUGUEV, N. V. LUGUEVA, V. V. SOKOLOV and YU. N. MALOVITSKII, *Inorg. Mater.* **21** (1985) 762.
78. F. K. VOLYNETS, G. N. DRONOVA, N. V. VEKSHINA and I. A. MIRONOV, *ibid.* **13** (1977) 432.
79. E. M. LOGINOVA, A. A. GRIZIK, N. M. PONOMAREV and A. A. ELISEEV, *ibid.* **11** (1975) 644.
80. J. FLAHAUT, LOUIS DOMANGE and MADELINE PATRIE, *Bull. Soc. Chim.* (1962) 2048.
81. J. F. NAKAHARA, M. J. TSCHETTER and B. J. BEAUDRY, T. TAKESHITA and K. A. GSCHNEIDNER Jr. in "Sixth International Conference on Thermoelectric Energy Conversion", The University of Texas at Arlington, edited by K. R. Rao, 12–14 March (University of Texas, Arlington, 1986) p. 35.
82. K. IKEDA, T. FURUYAMA, A. MAEDA, K. A. GSCHNEIDNER Jr, and B. J. BEAUDRY, *J. Phys. Soc. Jpn* **55** (1986) 2473.
83. K. IKEDA, K. A. GSCHNEIDNER Jr, B. J. BEAUDRY and U. ATZMONY, *Phys. Rev. B* **25** (1982) 4604.
84. K. IKEDA, K. A. GSCHNEIDNER Jr, B. J. BEAUDRY and T. ITO, *ibid.* **25** (1982) 4618.
85. T. TAKESHITA, K. A. GSCHNEIDNER Jr and B. J. BEAUDRY, in "Proceedings of the 5th International Conference on Thermoelectric Energy Conversion", The University of Texas, Arlington. Edited by K. R. Rao, 14–16 March, 1984. (The University of Texas, Arlington, 1984) p. 144.
86. K. A. GSCHNEIDNER Jr, B. J. BEAUDRY, T. TAKESHITA and S. S. EUCKER, S. M. A. TAHER, J. C. HO and J. B. GRUBER, *Phys. Rev. B* **24** (1981) 7187.
87. J. C. HO, S. M. A. TAHER, G. B. KING, J. B. GRUBER, B. J. BEAUDRY and K. A. GSCHNEIDNER Jr, *J. de Phys.* **39** (1978) C6-840.
88. J. F. NAKAHARA, B. J. BEAUDRY, K. A. GSCHNEIDNER Jr and T. TAKESHITA, *Mater. Res. Soc. Proc.* **97** (1987) 379.
89. J. F. NAKAHARA, T. TAKESHITA, M. J. TSCHETTER, B. J. BEAUDRY and K. A. GSCHNEIDNER Jr, *J. Appl. Phys.* **63** (1988) 2331.
90. *Idem*, in "The First European Conference on Thermoelectrics", Edited by D. M. Rowe (Peter Peregrinus, London, 1988) Ch. 14, p. 161.
91. A. A. KAMARZIN, K. E. MIRONOV, V. V. SOKOLOV, TU. N. MAOVITSKY and I. G. VASIL'YEVA, *J.Crystal Growth* **52** (1981) 619.
92. A. ADDAMIANO and P. A. DELL, *J. Phys. Chem.* **61** (1957) 1020.
93. A. ADDAMIANO and M. AVEN, *J. Appl. Phys.* **31** (1960) 36.
94. E. D. EASTMAN, L. BREWER, LE ROY A. BROMLEY, P. W. GILLES and NORMAN L. LOFGREN, *J. Am. Ceram. Soc.* **72** (1950) 4019.
95. W. GEFFCKEN and E. BERGER, Ger. Pat. 736411, May 1939.
96. R. ROY, *J. Am. Ceram. Soc.* **52** (1969) 344.
97. H. DISLICH, *Angew Chem.* **83** (1971) 428.
98. H. SCHMIDT, *J. Non-Cryst. Solids* **100** (1988) 51.
99. C. J. BRINKER, *J. Am. Ceram. Soc.* **65** (1982) C-4.
100. C. G. PANTANO, P. M. GLASER and D. J. ARMBRIGHT, in "Ultrastructure Processing of Ceramics, Glasses and Composites", edited by L. Hench and D. R. Ulrich (Wiley, New York, 1984) p. 161.
101. M. GUGLIELMI and G. CARTURAN, *J. Non-Cryst. Solids* **100** (1988) 16.
102. S. SAKKA and K. KAMIYA, *ibid.* **42** (1980) 403.
103. E. M. RABINOVICH, *J. Mater. Sci.* **20** (1985) 4259.
104. E. M. RABINOVICH, D. W. JOHNSON Jr, J. B. MACHESNEY and E. M. VOGEL, *J. Am. Ceram. Soc.* **66** (1983) 683.
105. R. K. ILER, in "Science of Ceramic Chemical Processing", edited by L. L. Hench and D. R. Ulrich (John Wiley, New York, 1986) p. 3.
106. C. J. BRINKER and G. W. SCHERER, in "Ultrastructure Processing of Ceramics, Glasses and Composites", edited by L. L. Hench and D. R. Ulrich (Wiley, New York, 1984) p. 43.
107. G. W. SCHERER, *J. Non-Cryst. Solids* **100** (1988) 77.
108. P. F. JAMES, *ibid.* **100** (1988) 93.
109. C. SANCHEZ, J. LIVAGE, M. HENRY and F. BABONNEAU, *ibid.* **100** (1988) 65.
110. L. L. HENCH, in "Science of Ceramic Chemical Processing", edited by L. L. Hench and D. R. Ulrich (John Wiley, New York, 1982) p. 52.
111. C. SANCHEZ, F. BABONNEAU, S. DOEUFF and A. LEAUSTIC, in "Ultrastructure Processing of Ceramics, Glasses and Composites", edited by L. L. Hench and D. R. Ulrich (Wiley, New York, 1988) p. 77.
112. Y. OZAKI, *Ferroelectrics* **49** (1983) 285.
113. S. S. FLASCHEN, *J. Am. Chem. Soc.* **77** (1955) 6194.
114. P. P. PHULÉ, Ph D dissertation, University of Arizona (1989).
115. P. J. MELLING, *Ceram. Bull.* **63** (1984) 1427.
116. E. MATIJEVIC and D. M. WILHELMY, *J. Coll. Interface Sci.* **86** (1982) 476.

117. J. D. MACKENZIE, *J. Non-Cryst. Solids* **100** (1988) 162.
118. S. SAKKA, in "Treatise on Materials Science and Technology", Vol. 22, edited by M. Tomozawa and R. H. Doremus (Academic Press, New York, 1982) p. 129.
119. G. W. SCHERER, *Yogyo Kyokai Shi* **95** (1987) 21.
120. C. J. BRINKER and G. W. SCHERER, in "Ultrastructure Processing of Ceramics, Glasses and Composites", edited by L. Hench and D. R. Ulrich (Wiley, New York, 1984) p. 43.
121. C. J. BRINKER and G. W. SCHERER, *J. Non-Cryst. Solids* **70** (1985) 301.
122. C. J. BRINKER, E. P. ROTH, G. W. SCHERER and D. R. TALLANT, *ibid.* **71** (1985) 171.
123. *Idem, ibid.* **72** (1985) 345.
124. C. J. BRINKER, G. W. SCHERER and E. P. ROTH, *ibid.* **72** (1985) 369.
125. C. J. BRINKER, W. D. DROTNING and G. W. SCHERER, in "Better Ceramics Through Chemistry", Vol. 32, Proceedings of the Materials Research Society Symposium, Albuquerque, New Mexico. Edited by C. J. Brinker, D. E. Clark and D. R. Ulrich (North Holland, New York, 1984) p. 25.
126. J. ZARZYCKI, in "Glass Science and Technology", Vol.2, edited by D. R. Uhlmann and N. J. Kriedl (Academic Press, New York, 1984) Ch. 7.
127. D. R. ULRICH, *J. Non-Cryst. Solids* **100** (1988) 174.
128. G. L. MESSING, S. HIRANO and H. HAUSNER (eds), "Ceramic Powder Science III", Ceramic Transactions, Vol. 12. Proceedings of the 3rd International Conference on Powder Processing Science, San Diego, 4–6 February 1990, and relevant papers in this volume (The American Ceramic Society, Ohio, 1990).
129. K. OSSEO-ASARE and F. J. ARRIAGADA, *ibid.* p. 3 and references 4-9 under Table I, p. 8.
130. H. W. LAVERENZ, "An Introduction to Luminescence of Solids" (Wiley, New York, 1950) p. 473.
131. C. E. JOHNSON, D. K. HICKEY and D. C. HARRIS, *Proc. SPIE* **683** (1986) 112.
132. T. A. GUITON, C. L. CZEKAJ, M. S. RAU, G. L. GEOFFROY and C. G. PANTANO, in "Better Ceramics Through Chemistry III", Vol. 121, Proceedings of the Materials Research Society, edited by C. J. Brinker, D. E. Clark and D. R. Ulrich (Material Research Society, 1988) 503.
133. T. A. GUITON, C. L. CZEKAJ and C. G. PANTANO, *J. Non-Cryst. Solids* **121** (1990) 7.
134. C. E. JOHNSON, D. C. HARRIS and C. B. WILLINGHAM, *Chem. Mater.* **2** (1990) 141.
135. M. AKINC and A. CELIKKAYA, in "Ceramic Powder Science III", edited by G. L. Messing, S. Hirano and H. Hausner, Ceramic Transactions, Vol. 12, Proceedings of the 3rd International Conference on Powder Processing Science, held in San Diego, 4–6 February 1990 (The American Ceramic Society, Ohio, 1990) p. 137.
136. A. BENSALEM and D. M. SCHLEICH, *Mater. Res. Bull.* **23** (1988) 857.
137. P. N. KUMTA, P. P. PHULÉ and S. H. RISBUD, *Mater Lett.* **5** (1987) 401.
138. C. M. VAUGHAN and W. B. WHITE, *Mater Res. Soc. Symp. Proc.* **97** (1987) 397.
139. L. H. WANG, M. H. HON, W. L. HUANG and W. Y. LIN, *Mater Sci. Eng.* **B7** (1990) 237.
140. *Idem, Mater Res. Bull.* **26** (1991) 649.
141. *Idem, J. Mater. Sci.* **26** (1991) 5013.
142. Y. HAN and M. AKINC, *J. Am. Ceram. Soc.* **74** (1991) 2815.
143. L. H. WANG, *J. Mater. Sci. Lett.* **12** (1993) 212.
144. S. H. HAN, K. A. GSCHNEIDNER Jr and B. J. BEAUDRY, *Scripta Metall. Mater.* **25** (1991) 295.
145. *Idem, J. Alloys & Compounds* **181** (1992) 463.
146. D. S. KNIGHT and W. B. WHITE, *Spectrochim. Acta* **46A** (1990) 381.
147. P. L. PROVENZANO and W. B. WHITE, *Chem. Phys. Lett.* **185** (1991) 117.
148. *Idem, J. Am. Ceram. Soc.* **73** (1990) 1766.
149. W. B. WHITE, *Proc. SPIE* **1326** (1990) 80.
150. R. BERMAN, in "The Properties of Diamond", edited by J. E. Field (Academic Press, London, 1979) Ch. 1.
151. A. T. COLLINS, *Proc. Mater. Res. Soc. Symp* **162** (1990) 3.
152. M. P. NADLER, C. K. LOWE-MA and T. A. VANDERAH, *Mater. Res. Bull.* submitted.
153. C. K. LOWE-MA, D. O. KIPP and T. A. VANDERAH, in "Long Wavelength Semiconductor Devices, Materials and Processes", edited by A. Katz, R. M. Biefield, R. L. Gunshar, R. J. Malik. *Mater. Res. Soc. Symp. Proc.* **216** (The Materials Research Society, 1991) p. 397.

Received 21 October 1992
and accepted 14 June 1993